·TOPICS ON CARDIOVASCULAR AND CEREBROVASCULAR DISEASES·
·心脑血管疾病专题·

In-depth analysis of retinal RNA transcriptome sequencing in a rat model of hypertensive retinopathy

SHI Wen[1,2], XIAO Shiyuan[1,2], BU Bing[1,2], HUANG Tianxin[1,2], JIANG Yiran[1,2], JIANG Wenmin[1,2]

(1. Department of Ophthalmology, Second Xiangya Hospital, Central South University, Changsha 410011;
2. Hunan Provincial Clinical Medicine Research Centre for Ophthalmic Disease, Changsha 410011, China)

ABSTRACT

Objective: Hypertensive retinopathy is a microvascular complication caused by systemic hypertension and can lead to severe visual impairment. At present, the molecular mechanisms of this disease remain incompletely understood, particularly the global expression profiles and regulatory networks of non-coding RNA (ncRNA). This study aims to comprehensively analyze the genome-wide differential expression profiles of messenger RNA (mRNA), microRNA (miRNA), long non-coding RNA (lncRNA), and circular RNA (circRNA) in retinal tissues from a spontaneously hypertensive rat (SHR) model of hypertensive retinopathy, and to observe transcriptomic changes after treatment with the calcium channel blocker lacidipine, thereby revealing their potential roles in disease pathogenesis and identifying possible therapeutic targets.

Methods: SHRs were used as a model of hypertensive retinopathy, and normotensive Wistar-Kyoto (WKY) rats were used as controls. Rats were divided into 3 groups: A control group (WKY), a model group (SHR), and a treatment group (SHR+lacidipine). Rats in the treatment group received lacidipine by gavage at 0.5 mg/(kg·d) for 8 consecutive weeks. At the end of the experiment, retinal tissues were collected for histopathological examination by hematoxylin and eosin (HE) staining and for high-throughput sequencing. The lncRNA library was used to analyze mRNA, lncRNA, and circRNA expression profiles, and the small RNA (sRNA) library was used to analyze miRNA expression profiles. Differential expression analysis was performed using DESeq2. The screening criteria were $|\log_2$ fold change (FC)$| \geq 1$ and false discovery rate (FDR) significance criteria for mRNAs and lncRNAs, and $|\log_2 FC| \geq 1$ and $P<0.05$ for miRNAs and circRNAs as exploratory candidates. Differentially expressed RNAs were subjected to Gene Ontology (GO) functional annotation and Kyoto Encyclopedia of Genes and Genomes (KEGG) pathway enrichment analysis. Competing endogenous RNA (ceRNA) regulatory networks involving

Date of reception: 2025-09-15
First author: SHI Wen, Email: 2209080111@csu.edu.cn, ORCID: 0000-0003-0398-591X
Corresponding author: JIANG Wenmin, professor, Email: wenminjiang@csu.edu.cn, ORCID: 0000-0003-4441-3379
Foundation item: This work was supported by the National Natural Science Foundation (81700838), the Natural Science Foundation of Hunan Province (2020JJ4789, 2025JJ50538), and the Natural Science Foundation of Changsha City (kq2403090), China.
Open access: This is an open access article under Creative Commons Attribution-NonCommercial-NoDerivatives 4.0 International (CC BY-NC-ND 4.0) (https://creativecommons.org/licenses/by-nc-nd/4.0/).

©Journal of Central South University (Medical Science). All rights reserved.

lncRNA/circRNA-miRNA-mRNA were constructed through target prediction and co-expression analysis. Ten mRNAs whose expression changes were reversed after treatment were selected for validation by real-time reverse transcription polymerase chain reaction (real-time RT-PCR; n=6 per group). Comparisons among multiple groups were performed using one-way analysis of variance and post hoc multiple-comparison tests.

Results: 1) Verification of the animal model: Blood pressure was significantly higher in the model group than in the control group. The model group exhibited edema of the retinal nerve fiber layer, dilation of vascular lumens, and increased retinal thickness. Lacidipine treatment reduced blood pressure and alleviated these pathological changes. 2) Differential expression of mRNAs: Compared with the control group, 870 mRNAs were significantly downregulated and 1 018 mRNAs were significantly upregulated in the model group. Compared with the model group, 2 644 mRNAs were significantly downregulated and 186 mRNAs were significantly upregulated in the treatment group. GO analysis showed that upregulated mRNAs in the model group were enriched in immune-inflammatory processes, such as leukocyte activation, chemotaxis, defense response, and regulation of tumor necrosis factor (TNF) production, whereas downregulated mRNAs were enriched in G protein-coupled receptor (GPCR) signaling, glycoprotein synthesis, ion channel activity, and related processes. KEGG analysis revealed that upregulated mRNAs in the model group were enriched in interleukin-17 (IL-17), TNF, oxidative stress, and lipid inflammatory mediator metabolic pathways, whereas downregulated mRNAs were enriched in phosphatidylinositol 3-kinase (PI3K) -protein kinase B (AKT) signaling, vascular smooth muscle contraction, extracellular matrix (ECM) -receptor interaction, and related pathways. In the treatment group, the downregulated mRNAs were mainly enriched in pathways related to immune-inflammatory activation, such as mast cell degranulation and leukocyte degranulation. 3) Treatment-reversed mRNAs: A total of 67 genes that were upregulated in the model group and downregulated after treatment were identified; these genes were mainly enriched in endoplasmic reticulum stress-associated apoptotic signaling, mitophagy, ubiquitin ligase activity, and related processes. In addition, 54 genes that were downregulated in the model group and upregulated after treatment were identified; these genes were mainly enriched in amino acid transport, integrin complex, focal adhesion, glutamate transport activity, and related processes. Real-time RT-PCR validated the expression changes of *Med22*, *Rmt1*, *Sytl3*, *Itgb7*, and *Slc1a3* which were decreased in the model group and increased after treatment, as well as *Rnf183*, *Lrrc29*, *Lat2*, *Hist1h4m*, and *Dpm3*, which were increased in the model group and decreased after treatment. These findings were consistent with the sequencing results. 4) Differential expression of miRNAs: Compared with the control group, 30 miRNAs were downregulated and 26 miRNAs were upregulated in the model group. Compared with the model group, 14 miRNAs were downregulated and 53 miRNAs were upregulated in the treatment group. Treatment-reversed miRNAs were identified: Rno-miR-1-3p, novel_miR_1203, and novel_miR_1417 were upregulated in the model group and downregulated after treatment, whereas novel_miR_107 and novel_miR_905 were downregulated in the model group and upregulated after treatment. Their target genes were enriched in regulation of retinal cone/rod cell differentiation, ECM remodeling, the Notch pathway, fatty acid synthesis, and related processes. 5) Differential expression of lncRNAs: Compared with the control group,

©Journal of Central South University (Medical Science). All rights reserved.

786 lncRNAs were downregulated and 764 lncRNAs were upregulated in the model group. Compared with the model group, 217 lncRNAs were downregulated and 230 lncRNAs were upregulated in the treatment group. A total of 55 lncRNAs that were upregulated in the model group and downregulated after treatment, and 76 lncRNAs that were downregulated in the model group and upregulated after treatment, were identified. Their target genes were enriched in immune regulation, wound healing, vascular remodeling, retinol metabolism related to rod-mediated scotopic vision, glutamatergic neuron differentiation, the forkhead box O (FoxO) pathway, retinoic acid-inducible gene I (RIG-I)-like receptor signaling, and related processes. 6) Differential expression of circRNAs: Compared with the control group, 45 circRNAs were downregulated and 47 circRNAs were upregulated in the model group. Compared with the model group, 25 circRNAs were downregulated and 22 circRNAs were upregulated in the treatment group. Eleven circRNAs that were downregulated in the model group and upregulated after treatment, and 10 circRNAs that were upregulated in the model group and downregulated after treatment, were identified. Their host genes were enriched in regulation of synaptic neural signaling, second messenger transmission, calcium signaling, and vascular endothelial growth factor (VEGF) signaling pathways. 7) Construction of ceRNA networks: Based on expression patterns and target prediction, multiple lncRNA/circRNA-miRNA-mRNA regulatory networks were constructed. For example, the networks composed of rno_circ_Rims2_10, rno-miR-1-3p, and related mRNAs, such as *Mmp14* and *Fasn*, as well as the novel_miR_1417 related network, may be involved in retinal stress responses, inflammatory regulation, and neurovascular remodeling.

Conclusion: This study is the first to integrate and analyze retinal transcriptomic profiles of mRNAs, miRNAs, lncRNAs, and circRNAs in an SHR model of hypertensive retinopathy, and it reveals RNA expression changes associated with lacidipine treatment. The results suggest that immune-inflammatory activation, neurovascular dysfunction, and ncRNA-mediated ceRNA regulatory networks may participate in the pathogenesis of hypertensive retinopathy. The identified differentially expressed molecules and predicted regulatory axes provide a candidate molecular basis for further mechanistic validation and screening of potential therapeutic targets.

KEY WORDS hypertensive retinopathy; high-throughput sequencing; differentially expressed RNA; non-coding RNA; diagnostic biomarker; therapeutic target

高血压视网膜病变大鼠模型视网膜组织RNA转录组测序的深度解析

施雯[1,2]，肖诗缘[1,2]，卜冰[1,2]，黄天馨[1,2]，姜怡然[1,2]，姜文敏[1,2]

(1. 中南大学湘雅二医院眼科，长沙 410011；2. 湖南省眼科疾病临床医学研究中心，长沙 410011)

[摘 要] 目的： 高血压视网膜病变是全身性高血压引起的微血管并发症，可导致严重的视力损害。目前对该病的分子机制认识尚不全面，尤其是非编码RNA(non-coding RNA，ncRNA)在其中的整体表达谱及调控网络缺乏系统

©Journal of Central South University (Medical Science). All rights reserved.

研究。本研究旨在全面分析自发性高血压大鼠(spontaneously hypertensive rat，SHR)高血压视网膜病变模型视网膜组织中信使RNA(messenger RNA，mRNA)、微RNA(microRNA，miRNA)、长链非编码RNA(long non-coding RNA，lncRNA)和环状RNA(circular RNA，circRNA)的全基因组差异表达谱，并观察钙通道阻滞剂拉西地平治疗后的转录组变化，以揭示其参与疾病发病机制的潜在作用，并识别可能的治疗靶点。**方法**：采用SHR作为高血压视网膜病变模型，正常血压Wistar-Kyoto(WKY)大鼠作为对照组。将大鼠分为3组：对照组(WKY)、模型组(SHR)和治疗组(SHR+拉西地平)。治疗组给予拉西地平0.5 mg/(kg·d)灌胃，连续8周。实验结束时收集视网膜组织，分别进行苏木精-伊红(hematoxylin and eosin，HE)染色、病理组织学检查和高通量测序。lncRNA文库用于分析mRNA、lncRNA和circRNA表达谱，小RNA(small RNA，sRNA)文库用于分析miRNA表达谱。使用DESeq2进行差异表达分析，筛选标准：mRNA和lncRNA以$|\log_2$倍数变化(fold change，FC)$|\geq 1$且错误发现率(false discovery rate，FDR)<0.05；miRNA和circRNA以$|\log_2 FC|\geq 1$且$P<0.05$为探索性候选。对差异表达RNA进行基因本体(Gene Ontology，GO)功能注释和京都基因和基因组数据库(Kyoto Encyclopedia of Genes and Genomes，KEGG)信号通路富集分析。通过靶标预测和共表达分析构建lncRNA/circRNA-miRNA-mRNA的竞争性内源RNA(competing endogenous RNA，ceRNA)调控网络。选取10个治疗后逆转的mRNA进行实时反转录聚合酶链反应(real-time reverse transcription polymerase chain reaction，real-time RT-PCR)验证(每组6只)。多组间比较采用单因素方差分析及事后多重比较检验。**结果**：1)动物模型验证：模型组血压显著高于对照组，视网膜神经纤维层水肿、血管管腔扩张、视网膜厚度增加；拉西地平治疗后血压降低并减轻了上述病理改变。2)mRNA差异表达：与对照组相比，模型组有870个mRNA表达显著下调、1 018个mRNA表达显著上调；与模型组相比，治疗组有2 644个mRNA表达显著下调、186个mRNA表达显著上调。GO分析显示模型组上调mRNA富集于免疫炎症过程[如白细胞活化、趋化性、防御反应，肿瘤坏死因子(tumor necrosis factor，TNF)产生调节]，下调mRNA富集于G蛋白偶联受体(G protein-coupled receptor，GPCR)信号、糖蛋白合成、离子通道活性等。KEGG分析显示模型组上调mRNA富集于白细胞介素-17(interleukin-17，IL-17)、TNF、氧化应激及脂质炎症介质代谢通路；下调mRNA富集于磷脂酰肌醇3激酶(phosphatidylinositol 3-kinase，PI3K)-蛋白激酶B(protein kinase B，AKT)信号、血管平滑肌收缩、细胞外基质(extracellular matrix，ECM)-受体相互作用等通路。治疗组中下调的mRNA主要富集于免疫炎症激活相关通路(如肥大细胞脱颗粒、白细胞脱颗粒)。3)治疗逆转的mRNA：鉴定出67个在模型组上调、治疗后下调的基因(主要富集于内质网应激凋亡信号、线粒体自噬、泛素连接酶活性等)，以及54个在模型组下调、治疗后上调的基因(主要富集于氨基酸转运、整合素复合物、黏着斑、谷氨酸转运活性等)。Real-time RT-PCR验证了*Med22*、*Rmt1*、*Sytl3*、*Itgb7*、*Slc1a3*(模型组降低，治疗后升高)及*Rnf183*、*Lrrc29*、*Lat2*、*Hist1h4m*、*Dpm3*(模型组升高，治疗后降低)的表达变化，与测序结果一致。4)miRNA差异表达：与对照组相比，模型组有30个miRNA下调、26个miRNA上调；与模型组相比，治疗组有14个miRNA下调、53个miRNA上调。筛选出治疗逆转的miRNA：Rno-miR-1-3p、novel_miR_1203、novel_miR_1417在模型组上调、治疗后下调；novel_miR_107、novel_miR_905在模型组下调、治疗后上调。其靶基因富集于视网膜视锥/视杆细胞分化调节、ECM重塑、Notch通路及脂肪酸合成等。5)lncRNA差异表达：与对照组相比，模型组有786个lncRNA下调、764个上调；与模型组相比，治疗组有217个lncRNA下调、230个上调。筛选出55个模型组上调、治疗后下调的lncRNA和76个模型组下调、治疗后上调的lncRNA。其靶基因富集于免疫调节、伤口愈合、血管重塑、视黄醇代谢(视杆细胞暗视觉)、谷氨酸能神经元分化、叉头框蛋白O(forkhead box O，FoxO)通路、维A酸诱导基因I样受体信号等。6)circRNA差异表达：与对照组相比，模型组有45个circRNA下调、47个上调；与模型组相比，治疗组有25个circRNA下调、22个上调。筛选出11个模型下调/治疗后上调的circRNA和10个模型上调/治疗后下调的circRNA。其宿主基因富集于突触神经信号调节、第二信使传递、钙信号和血管内皮生长因子(vascular endothelial growth factor，VEGF)信号通路。7)ceRNA网络构建：基于表达模式和靶标预测，构建了多个lncRNA/circRNA-miRNA-mRNA调控网络。例如，rno_circ_Rims2_10与rno-miR-1-3p及相关mRNA(如*Mmp14*、*Fasn*)组成的网络，以及novel_miR_1417相关网络，可能参与视网膜应激反应、炎症调控和神经血管重塑。**结论**：本研究在SHR高血压视网膜病变模型中整合分析了mRNA、miRNA、lncRNA和circRNA的视网膜转录组图谱，并揭示了拉西地平治疗相关的RNA表达变化。结果提示，免疫炎症激活、神经血管功能紊乱及ncRNA介导的ceRNA调控网络可能参与高血压视网膜病变的发病机制。鉴定出的差异表达分子及预测的调控轴为进一步的机制验证和潜在治疗靶点筛选提供了候选分子基础。

[关键词] 高血压视网膜病变；高通量测序；差异表达RNA；非编码RNA；诊断生物标志物；治疗靶点

Hypertensive retinopathy is a complication of systemic hypertension that affects the retinal microvasculature and is characterized by retinal changes resulting from hypertension[1]. These changes include

©Journal of Central South University (Medical Science). All rights reserved.

generalized and focal narrowing of the retinal arterioles, arteriovenous nicking, retinal hemorrhages, cotton-wool spots, hard exudates, and, in severe cases, optic disc swelling[2]. The pathogenesis of hypertensive retinopathy is complex and multifactorial, involving both direct and indirect effects of hypertension on the retinal vasculature. Direct effects include mechanical stress on the vessel wall leading to endothelial dysfunction, while indirect effects are mediated through the renin-angiotensin-aldosterone system, oxidative stress, and inflammation[3]. Despite its prevalence, hypertensive retinopathy often remains unrecognized until it has progressed to a severe stage, highlighting the need for early detection and intervention[4].

The management of hypertensive retinopathy primarily involves controlling systemic blood pressure. However, recent advances in the molecular and cellular mechanisms underlying hypertensive retinopathy have opened new avenues for targeted therapy. Non-coding RNA (ncRNA) play a crucial role in the pathogenesis of hypertensive retinopathy and potential therapeutic targets[5-6]. NcRNAs are RNA molecules that do not code for proteins but exert critical effects on gene expression, modulating it at the transcriptional and post-transcriptional levels. MicroRNA (miRNA), long non-coding RNA (lncRNA), and circular RNA (circRNA) are among the most extensively studied ncRNAs[7]. Several studies[5, 8-9] have highlighted the importance of ncRNAs in hypertensive retinopathy. For instance, miRNAs, which are small ncRNAs that bind to the 3’ untranslated regions of target messenger RNA (mRNA) to modulate gene expression, could regulate endothelial function, inflammation, and vascular remodeling in hypertensive retinopathy. Similarly, lncRNAs longer than 200 nucleotides that can modulate gene expression through various mechanisms are differentially expressed in the retinas of hypertensive rats and may contribute to the pathogenesis of hypertensive retinopathy[6, 10]. Furthermore, circRNAs, which are covalently closed ncRNAs that act as miRNA sponges, have recently been identified as potential regulators of gene expression in hypertensive retinopathy[11-12]. Taken together, ncRNAs might serve as therapeutic targets for hypertensive retinopathy. Yet, there is little research on the comprehensive role of ncRNAs in hypertensive retinopathy to date. In particular, most available studies have focused on individual ncRNA classes or specific RNA molecules, whereas integrated profiling of miRNAs, lncRNAs, circRNAs, and their potential crosstalk with mRNAs remains limited in hypertensive retinopathy.

Considering the emerging role of ncRNAs in hypertensive retinopathy and the need for more effective therapeutic strategies, this research aims to identify key ncRNAs involved in the pathogenesis and treatment of hypertensive retinopathy. Spontaneously hypertensive rats (SHRs) were used as the model of hypertensive retinopathy, with or without treatment. High-throughput sequencing was performed on normal control rats and hypertensive retinopathy models, including those treated. A comprehensive analysis of the expression profiles of differentially expressed RNAs, including miRNAs, lncRNAs, and circRNAs, in these models was conducted. The miRNA target gene network, namely the competing endogenous RNA (ceRNA) regulatory network, was constructed and analyzed to identify potential crosstalk between ncRNAs and their target genes. Furthermore, Kyoto Encyclopedia of Genes and Genomes (KEGG) and Gene Ontology (GO) analyses were conducted to elucidate the functions of the identified ncRNAs and their target genes. This study aims to clarify the potential involvement of ncRNAs in hypertensive retinopathy and to identify candidate biomarkers and therapeutic targets.

1 Materials and methods

1.1 Ethics statement

All the animal experiments in this research have been approved by the Institutional Animal Care and Use Committee, the Second Xiangya Hospital, Central South University, and conformed to the ethical principles of experimental animal welfare (Approval number: 20230866).

1.2 Experimental animals and treatments

SHRs were used as the model of hypertensive retinopathy, with normotensive Wistar-Kyoto (WKY) rats serving as normal controls. Male rats were used in the present study. All animals were purchased from Charles River Laboratories (Beijing, China). The rats were adaptively housed under controlled temperature

©Journal of Central South University (Medical Science). All rights reserved.

and humidity with a 12-h light/dark cycle before the experiment. The experiment started when the rats were 5 weeks old. The rats were assigned to 3 groups: A control group, a model group, and a treated group (6 rats in each). The control group consisted of WKY rats, whereas the model and treated groups consisted of SHRs. Rats in the control and model groups were maintained under standard conditions for 8 weeks. In contrast, rats in the treated group received lacidipine through oral gavage at a dose of 0.5 mg/(kg·d) for 8 consecutive weeks. The blood pressure was monitored every week using tail-cuff plethysmography. Rats were placed in a restrainer and allowed to acclimate for at least 1 min before measurements were taken. The systolic blood pressure was measured 3 times consecutively, and the average value was used for analysis. At the end of the experiment, the rats were 13 weeks old and were sacrificed by an overdose of intraperitoneal ketamine and xylazine. For each animal, the left eyeball was used for histopathological examination, and the right eyeball was used for RNA extraction and sequencing. RNA sequencing was performed using 3 independent biological replicates per group, and no pooled samples were used. For real-time reverse transcription polymerase chain reaction (real-time RT-PCR) validation, 6 independent biological replicates per group were used. The sample size for sequencing was selected based on the exploratory nature of transcriptomic profiling and on common practice in high-throughput sequencing studies of animal tissues.

1.3 Histopathological examination

After being fixed in 4% paraformaldehyde overnight and paraffin-embedded, the eyeballs used for pathological analysis were sliced at a thickness of 5 μm. Changes in retinal tissues were observed as previously described by staining the slices with hematoxylin and eosin (HE)[13].

1.4 High-throughput sequencing

For RNA quantification, RNA degradation and contamination were examined using 1.5% agarose gels. The NanoDrop 2000 Spectrophotometer (Thermo Fisher Scientific, Wilmington, DE) was used to measure RNA content and purity. The RNA Nano 6000 Assay Kit of the Agilent Bioanalyzer 2100 System (Agilent Technologies, CA, USA) was used to assess RNA integrity. Retinal tissues from individual animals were used for RNA extraction, and no pooled samples were used. Three independent biological replicates were included in each group for sequencing.

For each sample, 1.5 μg of RNA was used as input for lncRNA library preparation and sequencing, and the Ribo-Zero™ ribosomal RNA (rRNA) Removal Kit (Epicenter, USA) was used to remove rRNA. The NEBNext® Ultra™ Directional RNA Library Prep Kit for Illumina (NEB, USA) was used according to the manufacturer's protocol to generate sequencing libraries, and index codes were added to assign sequences to each sample. The lncRNA libraries were used to analyze mRNA, lncRNA, and circRNA expression profiles on the Illumina HiSeq platform (Illumina, USA).

For each sample, 2.5 ng of RNA was used as input material for sRNA library preparation and sequencing. The NEBNext® small RNA Sample Library Prep Kit for Illumina (NEB, USA) was used according to the manufacturer's protocol to generate sequencing libraries, and index codes were added to assign sequences to each sample. The sRNA libraries were used to analyze miRNA expression profiles on the Illumina HiSeq platform. Raw sequencing reads (raw reads) were first processed using in-house Perl scripts according to the following quality control standards: Reads containing sequencing adapters were removed; reads with an N content greater than 10% were removed; low-quality reads were removed by defining a base with *Q*-score ≤10 as a low-quality base, and a read was discarded when the proportion of low-quality bases reached ≥50% of the total read length. For lncRNA, mRNA, and circRNA data, high-quality clean reads were obtained directly after the above common filtering steps. For miRNA data, after the common quality control steps, reads with lengths <15 nt or >35 nt were further discarded to retain mature miRNA fragments (typically 18－35 nt in length). The *Q*20, *Q*30, and GC content of all clean reads were calculated, with *Q*20≥ 95% and *Q*30≥90% as the thresholds for acceptable data quality. All downstream analyses were based on high-quality clean reads. Clean reads were subsequently mapped to the rat reference genome Rattus norvegicus Rnor_6.0 (GCA_000001895.4) using HISAT2 software and assembled into transcripts using StringTie software.

©Journal of Central South University (Medical Science). All rights reserved.

1.5 LncRNA, circRNA, and miRNA identification and expression analysis

For mRNA analysis, gene expression levels were quantified as fragments per kilobase of exon per million mapped fragments (FPKM), and differential expression analysis was performed using DESeq2 in the R language. The threshold of $|\log_2$ fold change (FC)$| >1$ was selected to identify transcripts with at least a two-fold expression difference, thereby focusing downstream functional enrichment and network analyses on RNAs with more pronounced expression changes. Significantly differentially expressed mRNAs were screened using $|\log_2 FC| \geqslant 1$ and false discovery rate (FDR) <0.05.

For lncRNA analysis, four computational approaches [coding potential calculator (CPC), coding-non-coding index (CNCI), Pfam, and coding-potential assessment tool (CPAT)] were combined to filter non-protein-coding RNA candidates, and transcripts with a length >200 nt and containing at least 2 exons were selected as lncRNA candidates, which were further classified into long intergenic noncoding RNA (lincRNA), intronic lncRNA, antisense lncRNA, and sense lncRNA using gffcompare. LncRNA expression levels were quantified as FPKM. Differential expression analysis was performed using the DESeq2 R package, with $|\log_2 FC| \geqslant 1$ and FDR<0.05 as the threshold.

For circRNA identification, CIRI v2.0 and find_circ were used in combination, and the intersection of the results from both methods was taken as the final prediction. CIRI detects junction reads with paired chiastic clipping (PCC) signals and applies paired-end mapping and GT-AG splicing signals for filtering, while find_circ uses 20 bp anchor points from both ends of reads to identify back-spliced junctions with GT/AG signals. CircRNA expression levels were quantified and normalized using the spliced reads per billion mapped (SRPBM) algorithm. Differential expression analysis was performed using the DESeq2 R package, with $|\log_2 FC| \geqslant 1$ and $P<0.05$ (without FDR adjustment) as the threshold.

For miRNA analysis, clean reads were aligned to Silva, GtRNAdb, Rfam, and Repbase databases using Bowtie to filter out rRNA, transfer RNA, small nuclear RNA, small nucleolar RNA, and other ncRNAs. The remaining reads were compared with miRBase to detect known miRNAs and predict novel miRNAs, with secondary structures predicted by RNAfold. MiRNA expression levels were quantified by mapping sRNA reads back to precursor sequences to obtain read counts per miRNA. MiRNA expression levels were quantified and normalized using the transcripts per million (TPM) algorithm. Differential expression analysis was performed using the DESeq2 R package, with $|\log_2 FC| \geqslant 1$ and $P<0.05$ (without FDR adjustment) as the threshold.

Because strict FDR correction yielded very few or no miRNA and circRNA candidates for downstream network construction, miRNAs and circRNAs screened using a nominal $P<0.05$ were considered exploratory candidates, whereas mRNAs and lncRNAs screened using an FDR<0.05 were regarded as the primary differentially expressed RNA sets.

1.6 Co-expression analysis

The expression profiles of coding (mRNAs) and ncRNAs (miRNAs, lncRNAs, or circRNAs) were obtained from the transcriptome sequencing data. By analyzing the correlation between the expression levels of coding and ncRNAs, the potential interactions (circRNA-related miRNAs, lncRNA-related miRNAs, and miRNA-related mRNAs) were identified. Based on these correlations, the regulatory network was then established.

1.7 GO and KEGG analyses

Metascape[14] or the clusterProfiler package in R was employed to perform functional and pathway enrichment annotations of the identified ncRNAs and their target genes. The GO analysis provided information on the biological functions, cellular components, and molecular activities associated with these RNAs and genes. The KEGG analysis revealed the pathways in which these RNAs and genes are involved. The mRNAs in the network were analyzed using STRING, and a protein-protein interaction (PPI) network was established.

1.8 Establishment of circRNA/lncRNA-miRNA-mRNA ceRNA network

Potential interactions across circRNAs, lncRNAs, miRNAs, and mRNAs were predicted and analyzed. The miRNA target sites on circRNAs, lncRNAs, and mRNAs were predicted using a bioinformatics tool as follows: The Perl program was run with the TargetScan

©Journal of Central South University (Medical Science). All rights reserved.

(version 7.0) source code and the Strawberry Perl Platform for Windows to predict miRNA potential target sites in the given lncRNAs, circRNAs, and mRNA 3' untranslated regions. The circRNA/lncRNA-miRNA-mRNA interactions were then represented within a ceRNA network. For the construction of the ceRNA network, a more inclusive threshold was applied to identify candidate mRNAs. Specifically, mRNAs with $|\log_2 FC| > 0.4$ and FDR ≤0.05 were included, while the criteria for lncRNAs, circRNAs, and miRNAs remained consistent with those described above.

1.9 Real-time RT-PCR

To validate the reliability of the sequencing data, 10 treatment-reversed mRNAs (5 that were upregulated in the model but downregulated in the treated group, and 5 that were downregulated in the model group but upregulated in the treated group) with functional annotation and large FCs were selected from the intersected differentially expressed mRNA sets for analysis. These genes comprised *Med22*, *Rmt1*, *Sytl3*, *Itgb7*, *Slc1a3*, *Rnf183*, *Lrrc29*, *Lat2*, *Hist1h4m*, and *Dpm3*. The sequences of all primers used for real-time RT-PCR are listed in Supplementary Table 1 (https://doi.org/10.57760/sciencedb.xbyxb.00168). Total RNA was extracted from retinal tissues of the control, model, and lacidipine-treated groups, with 6 biological replicates per group. After reverse transcription, real-time RT-PCR was performed using gene-specific primers. Relative mRNA expression levels were calculated using the $2^{-\Delta\Delta Ct}$ method, with glyceraldehyde-3-phosphate dehydrogenase (*GAPDH*) used as the internal reference gene.

1.10 Statistical analysis

Data are expressed as mean±standard deviation. The differences among 3 groups was analyzed by one-way analysis of variance (ANOVA) followed by post hoc multiple-comparison tests. $P<0.05$ was considered statistically significant.

2 Results

2.1 Verification of animal models and procedures of bioinformatics analyses

Before transcriptome sequencing, blood pressure and retinal histopathological changes were examined to verify the establishment of the hypertensive retinopathy model and the effect of lacidipine treatment. Compared with the control group, the model group showed elevated blood pressure ($P<0.01$). In contrast, lacidipine treatment reduced blood pressure in the treated group ($P<0.01$, Figure 1A). HE staining results showed that the retinas of rats in the model group showed edema in the nerve fiber layer, dilation of the vascular lumen, and increased retinal thickness. In contrast, these pathological changes were attenuated in the treated group (Figure 1B). Retinal thickness was significantly increased in the model group compared with the control group ($P<0.01$). In contrast, lacidipine treatment significantly reduced retinal thickness compared with the model group ($P<0.01$, Figure 1B). After confirming the pathological alterations, high-throughput sequencing was performed to characterize mRNA, miRNA, lncRNA, and circRNA expression profiles in retinal tissues from the 3 groups. Figure 1C shows the overall analytical workflow based on high-throughput sequencing data from the control, model, and treated groups. The workflow included RNA extraction and sequencing, differential expression analysis of mRNAs, miRNAs, lncRNAs, and circRNAs, functional enrichment analysis, identification of treatment-reversed RNAs, real-time RT-PCR validation of selected mRNAs, and construction of ceRNA regulatory networks.

2.2 Differentially expressed mRNAs among the control, model, and treated groups and related functions and signaling pathways

Principal component analysis (PCA) of the normalized mRNA expression matrix showed a clear separation among the control, model, and treated groups, indicating that the retinal transcriptomic profiles differed markedly across groups. The treated group showed a partial shift away from the model group, suggesting that lacidipine treatment partially reversed the transcriptomic alterations associated with hypertensive retinopathy (Supplementary Figure 1A, https://doi.org/10.57760/sciencedb.xbyxb.00168). The original matrix contained 43 468 mRNA transcripts. After filtering out low-expression mRNAs with a sum count ≤1 across all samples, 36 174 mRNAs were retained for downstream

©Journal of Central South University (Medical Science). All rights reserved.

analysis. Differential expression analysis of the normalized mRNA expression matrix was then conducted using DESeq2. The results showed that, compared with the control group, 870 mRNAs were significantly decreased ($log_2FC<-1$, adjusted $P<0.05$), and 1 018 mRNAs were significantly increased ($log_2FC>1$, adjusted $P<0.05$) in the model group (Figure 2A). Compared with the model group, 2 644 mRNAs were significantly decreased ($log_2FC<-1$, adjusted $P<0.05$), and 186 mRNAs were significantly increased ($log_2FC>1$, adjusted $P<0.05$) in the treated group (Figure 2B).

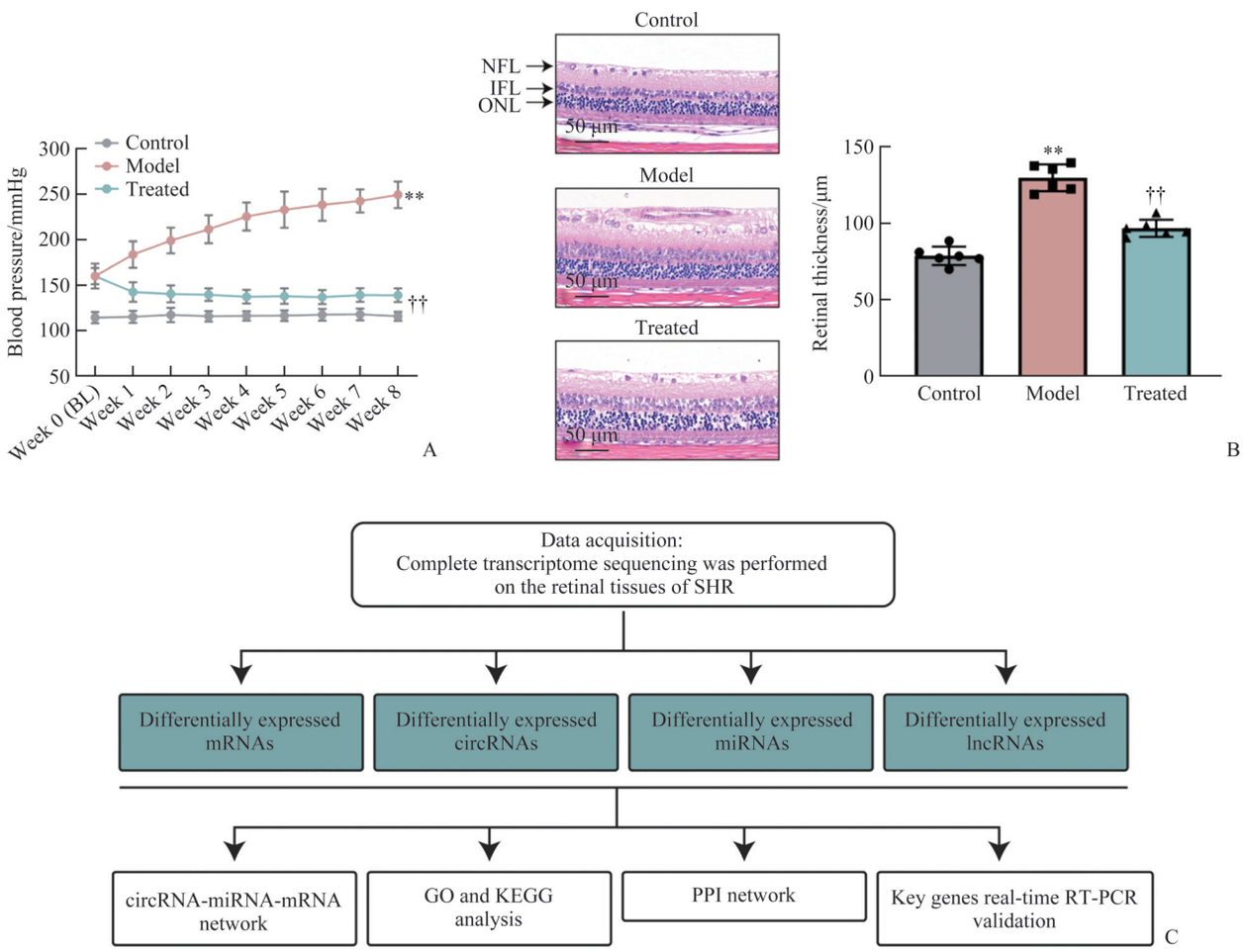

Figure 1 Verification of animal models and procedures of bioinformatics analyses

A: Blood pressure levels in the control, model, and treated groups during the experimental period. B: Histopathological features and retinal thickness analysis of retinal tissues from the control, model, and treated groups. C: Schematic workflow that shows the major steps of transcriptomic analysis, including sample collection, RNA sequencing, data filtering and quality control, differential expression analysis, ceRNA network construction, functional enrichment analysis, screening of treatment-reversed RNAs and validation (n=6). Data are expressed as mean±standard deviation. The between-group comparisons are made with an independent t-test. **$P<0.01$ vs the control group; ††$P<0.01$ vs the model group. NFL: Nerve fiber layer; INL: Inner nuclear layer; ONL: Outer nuclear layer; SHR: Spontaneously hypertensive rat; GO: Gene Ontology; KEGG: Kyoto Encyclopedia of Genes and Genomes; PPI: Protein-protein interaction; real-time RT-PCR: Real-time reverse transcription polymerase chain reaction; mRNA: Messenger RNA; miRNA: MicroRNA; lncRNA: Long non-coding RNA; circRNA: Circular RNA.

Next, GO functional enrichment analysis was performed on the 2 clusters of differentially expressed mRNAs. As shown in Supplementary Figure 1B (https://doi.org/10.57760/sciencedb.xbyxb.00168), the upregulated mRNAs in the hypertensive retinopathy models were mainly enriched in immune-inflammatory

©Journal of Central South University (Medical Science). All rights reserved.

processes, including cell killing, myeloid leukocyte activation, chemotaxis/taxis, defense response, and positive regulation of tumor necrosis factor (TNF) production, as well as extracellular matrix (ECM)-related components and immune receptor/chemokine activities. The downregulated mRNAs mainly affected G protein-coupled receptor signaling, protein glycosylation, and glycoprotein biosynthetic processes, as well as calcium channel complexes and ligand-gated ion channel or transmembrane transporter activities. The upregulated mRNAs within the treated group in comparison with the model group were mainly enriched in ion transport, especially sodium ion transmembrane transport, together with immune-related processes, cell migration, and membrane surface-specialized structure-related functions. The decreased mRNAs within the treated group were mainly enriched in immune-inflammatory activation, particularly mast cell- and leukocyte degranulation-related processes, together with membrane microdomain-, cell migration structure-, partial protein modification- and transport-related functions, suggesting that lacidipine treatment may partially suppress abnormally activated immune-inflammatory responses (Supplementary Figure 1C, https://doi.org/10.57760/sciencedb.xbyxb.00168).

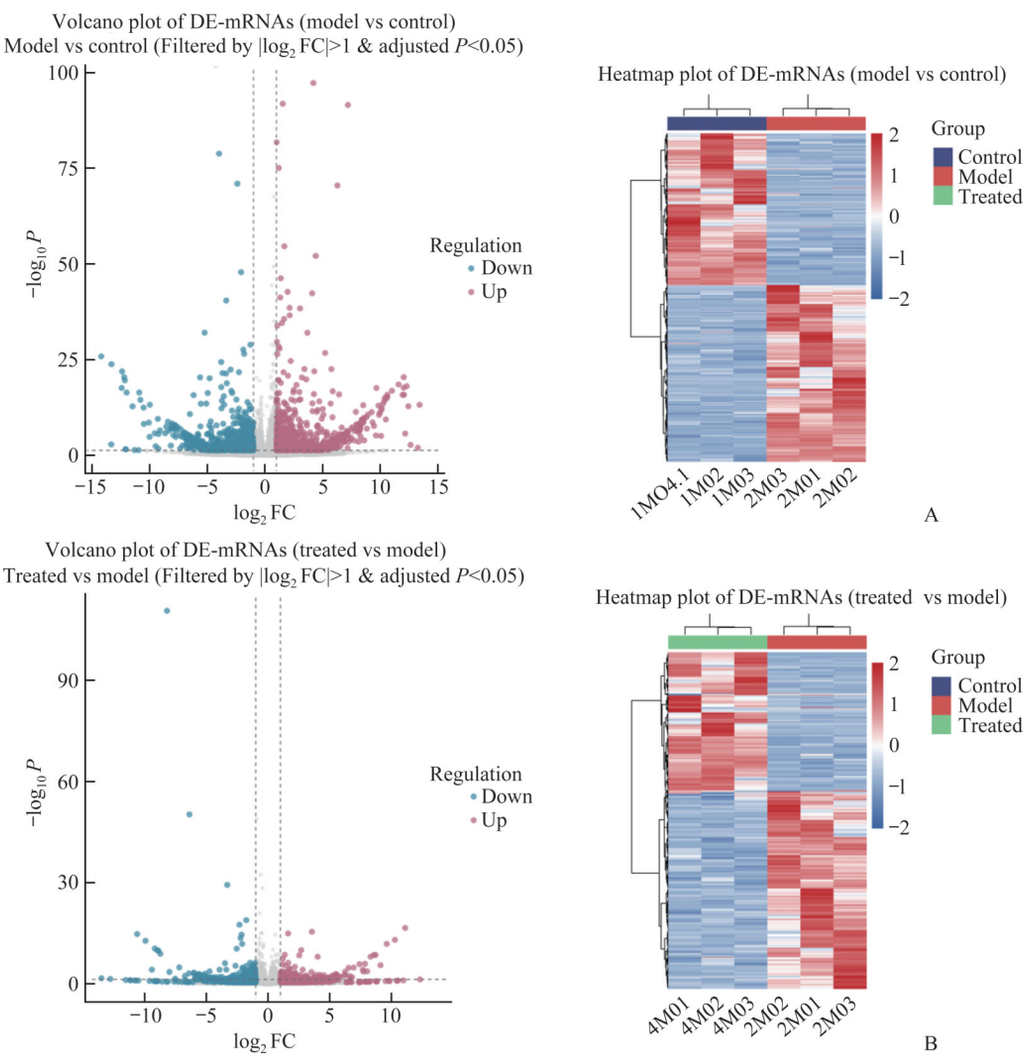

Figure 2 Differentially expressed mRNAs among groups

A: Differentially expressed mRNAs between the model and control groups are shown in the volcano plots and the hierarchical clustering heatmap. B: Differentially expressed mRNAs between the model and treated groups are shown in the volcano plots and the hierarchical clustering heatmap (n=3). Differentially expressed transcripts were screened using $|\log_2 FC|>1$ and adjusted $P<0.05$. DE-mRNA: Differentially expressed messenger RNA; FC: Fold change.

©Journal of Central South University (Medical Science). All rights reserved.

The KEGG signaling pathways enrichment annotation on differentially expressed mRNAs between the hypertensive retinopathy model and control groups revealed that the upregulated mRNAs primarily reflected changes within oxidative stress, inflammatory, and immune responses [interleukin-17 (IL-17), TNF signaling], lipid inflammatory mediator metabolism, and abnormal energy metabolism (Figure 3A). The downregulated mRNAs were enriched in the phosphoinositide 3-kinase (PI3K)-protein kinase B (AKT) signaling pathway, vascular smooth muscle contraction, ECM-receptor interaction, receptor-ligand interaction, metabolic transport, and detoxification-related pathways (cytochrome P450-associated signaling; Figure 3A). The increased mRNAs within the treated group in comparison with the model group were shown to be enriched in immune-cell migration and adhesion-related processes, inflammatory signaling regulation, and amino acid metabolism-related pathways, whereas those downregulated in the treated group were enriched in immune-inflammatory signaling, N-glycan biosynthesis, drug metabolism, and cardiac muscle contraction-related pathways (Figure 3B).

Hub genes in hypertensive retinopathy models and treatments were analyzed. Figure 4A shows that 67 genes were significantly increased in the model group compared with the control group. In contrast, they were significantly decreased in the treated group compared with the model group ($|\log_2FC| >1$, adjusted $P<0.05$) (Supplementary Table 2, https://doi.org/10.57760/sciencedb.xbyxb.00168). In addition, Figure 4B shows that 54 mRNAs were significantly downregulated in the model group compared with the control group, while significantly upregulated in the treated group compared with the model group (Supplementary Table 3, https://doi.org/10.57760/sciencedb.xbyxb.00168). These "model-up and treated-down" genes were mainly enriched in endoplasmic reticulum stress-related apoptotic signaling, mitochondrial protein localization, and mitophagy, ubiquitin ligase-related activities, and membrane- and organelle-associated components (Supplementary Figure 1D and 1E, https://doi.org/10.57760/sciencedb.xbyxb.00168). KEGG analysis further indicated their involvement in N-glycan biosynthesis, mitophagy, and natural killer cell-mediated cytotoxicity (Figure 4C). These "model-down and treated-up" genes were mainly enriched in amino acid transport and metabolism, especially aspartate/glutamate transport, intracellular sodium ion homeostasis, integrin complex, focal adhesion, cell-substrate junction, and glutamate transporter activity. KEGG analysis further linked these genes to the synaptic vesicle cycle, ECM-receptor interaction, glutamatergic synapse, integrin signaling, cell adhesion molecule interaction, neuroactive ligand signaling, focal adhesion, and transcriptional misregulation in cancer (Figure 4D).

2.3 Differentially expressed miRNAs and functional analysis among control, model, and treated groups

The original matrix contained 2 283 miRNA transcripts. After removal of low-abundance transcripts (sum count ⩽1 across all samples), 1 337 miRNAs were retained for downstream analysis. First, PCA showed a clear separation among the 3 groups based on miRNA expression profiles (Supplementary Figure 1F, https://doi.org/10.57760/sciencedb.xbyxb.00168). Differential expression analysis was then performed using DESeq2. Compared with the control group, 30 miRNAs were significantly decreased ($\log_2FC<-1$, $P<0.05$), while 26 were significantly increased ($\log_2FC>1$, $P<0.05$) within model group (Figure 5A). Compared with the model group, 14 miRNAs were significantly decreased ($\log_2FC<-1$, $P<0.05$), while 53 were significantly increased ($\log_2FC>1$, $P<0.05$) within the treated group (Figure 5B). The target genes of the differentially expressed miRNAs were predicted and applied for GO functional annotation. The targets of the differentially expressed miRNAs between the model group and control group were significantly enriched in GTPase activity, and those of miRNAs between the treated and model groups were mainly enriched in ion pathways, lysosomes, and chromatin-related functions (Supplementary Figure 1G and 1H, https://doi.org/10.57760/sciencedb.xbyxb.00168).

Next, the differentially expressed miRNAs between the hypertensive retinopathy model and treated groups were compared. MiRNAs downregulated in the hypertensive retinopathy model group (model-down) and upregulated in the treated groups (treated-up), and miRNAs upregulated in the hypertensive retinopathy model group (model-up) and downregulated in the

©Journal of Central South University (Medical Science). All rights reserved.

treated groups (treated-down) were selected. As shown in Supplementary Figure 2A (https://doi.org/10.57760/sciencedb.xbyxb.00168), 3 miRNAs (rno-miR-1-3p, novel_miR_1203, novel_miR_1417) were upregulated within the model group but significantly downregulated after treatment; 2 miRNAs (novel_miR_107, novel_miR_905) were downregulated within the model group but significantly upregulated after treatment ($|\log_2 FC|>1$, $P<0.05$). After predicting the target genes of these miRNAs, 160 targets were found to be associated with 4 miRNAs (rno-miR-1-3p, novel_miR_1203, novel_miR_905, and novel_miR_1417; Supplementary Figure 2B, https://doi.org/10.57760/sciencedb.xbyxb.00168). Among them, 34 were known protein-coding genes related to miRNAs novel_miR_1417, novel_miR_905, and novel_miR_1203 (Supplementary Figure 2C, https://doi.org/10.57760/sciencedb. xbyxb.00168).

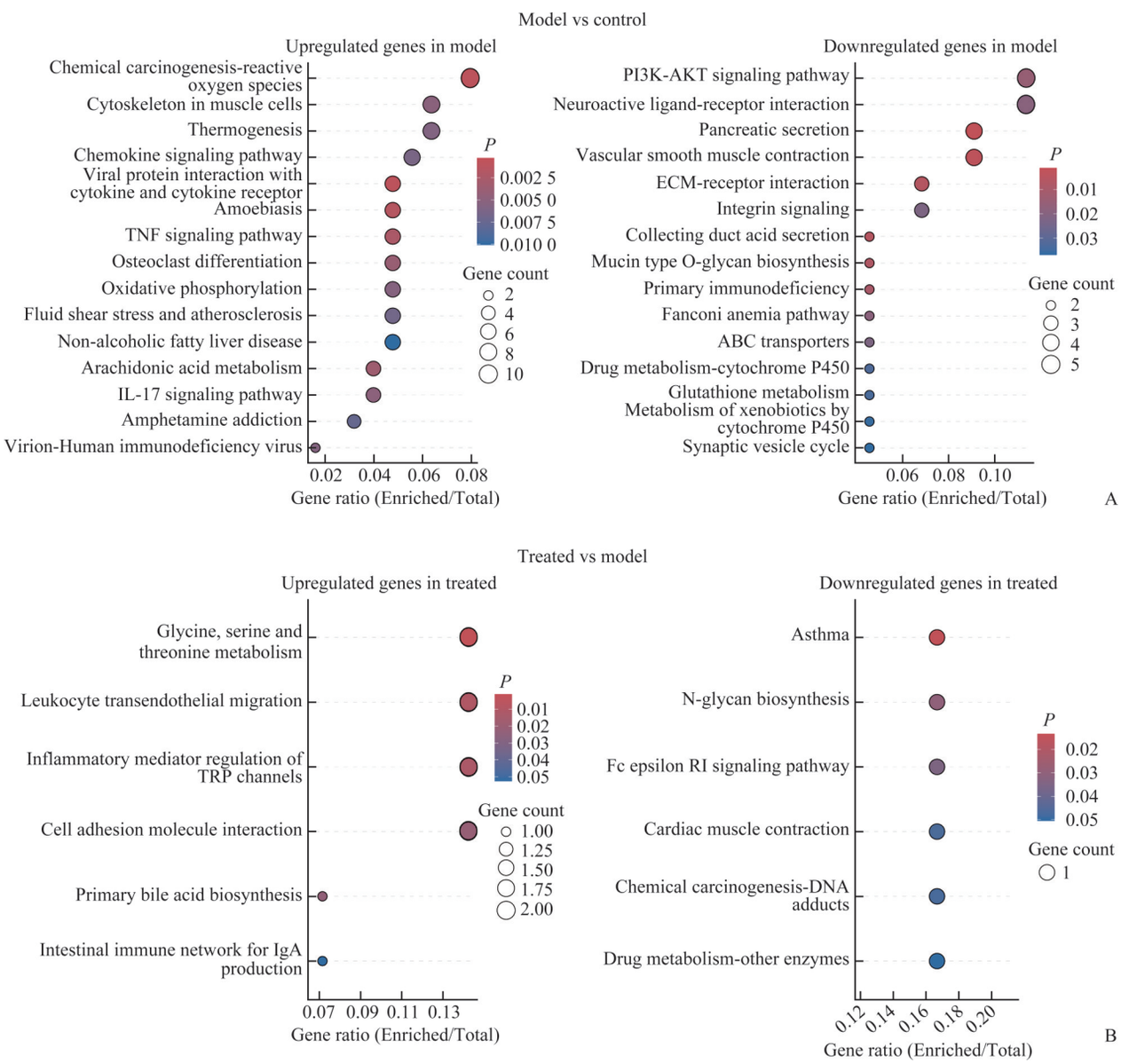

Figure 3 KEGG signaling pathway enrichment annotation on differentially expressed mRNAs among groups

A: KEGG signaling pathway enrichment annotation on differentially expressed mRNAs (upregulated and downregulated) between the hypertensive retinopathy model and control groups. B: KEGG signaling pathway enrichment annotation on differentially expressed mRNAs (upregulated and downregulated) between the model and treated groups. TNF: Tumor necrosis factor; IL-17: Interleukin-17; PI3K: Phosphoinositide 3-kinase; AKT: Protein kinase B; ECM: Extracellular matrix; IgA: Immunoglobulin A; ABC: ATP-binding cassette; TRP: Transient receptor potential.

©Journal of Central South University (Medical Science). All rights reserved.

The above target genes with known functions were used for GO functional annotation and KEGG signaling pathway annotation, and were significantly enriched in tissue organ formation (negative regulation of animal organ morphogenesis, positive modulation of myotube differentiation). They also participated in eye and retinal-related functions, such as the negative regulation of retinal cone cells, retinal rod cell fate commitment, and the regulation of retinal cone cells. In addition, pigment granule precipitation and ECM remodeling (collagen) were also observed. The KEGG enrichment analysis of miRNA target genes primarily involved cell adhesion, the Notch pathway, and fatty acid synthesis (Supplementary Figure 3, https://doi.org/10.57760/sciencedb.xbyxb.00168).

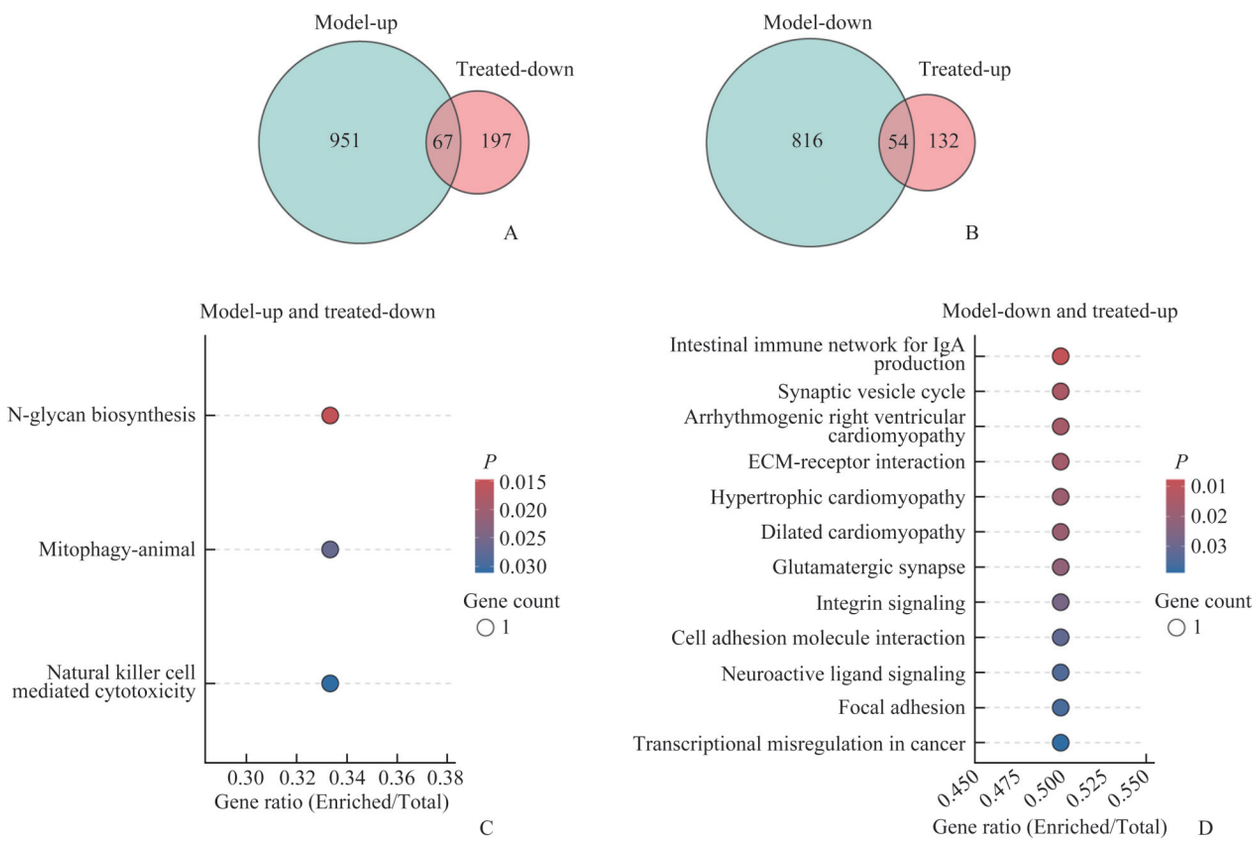

Figure 4 Hub genes of the hypertensive retinopathy and treatment

A and B: Differentially expressed RNAs between the hypertensive retinopathy model and treated groups were compared, and intersected genes were identified. Genes upregulated in the hypertensive retinopathy model group (model-up) and downregulated in the treated groups (treated-down; A), and genes downregulated in the model group (model-down) and upregulated in the treated groups (treated-up; B) were selected. C and D: The "model-up and treated-down" (C) and "model-down and treated-up" (D) genes were applied for the KEGG analyses.

2.4 Differentially expressed lncRNAs and functional analysis among control, model, and treated groups

The original matrix contained 59 080 lncRNA transcripts. After removal of low-abundance transcripts (sum count ⩽1 across all samples), 31 968 lncRNAs were retained for downstream analysis. PCA showed a clear separation among the 3 groups based on lncRNA expression profiles (Supplementary Figure 1I, https://doi.org/10.57760/sciencedb.xbyxb.00168). Differential expression analysis was then performed using DESeq2. The DESeq2 normalized expression matrix differential analysis (Supplementary Figure 4A−4C, https://doi.org/10.57760/sciencedb.xbyxb.00168) revealed that, comparing

©Journal of Central South University (Medical Science). All rights reserved.

with the control group, 786 downregulated lncRNAs ($log_2FC<-1$, adjusted $P<0.05$) and 764 upregulated lncRNAs ($log_2FC>1$, adjusted $P<0.05$) were found in the model group. Similarly, when comparing the model group, 217 downregulated lncRNAs ($log_2FC<-1$, adjusted $P<0.05$) and 230 dramatically upregulated lncRNAs ($log_2FC>1$, adjusted $P<0.05$) were observed in the treated group. After intersection, 55 lncRNAs were significantly increased within the model group than control group, while markedly decreased after treatment than the model group; 76 lncRNAs were significantly decreased within the model group than control group but significantly increased after treatment than the model group.

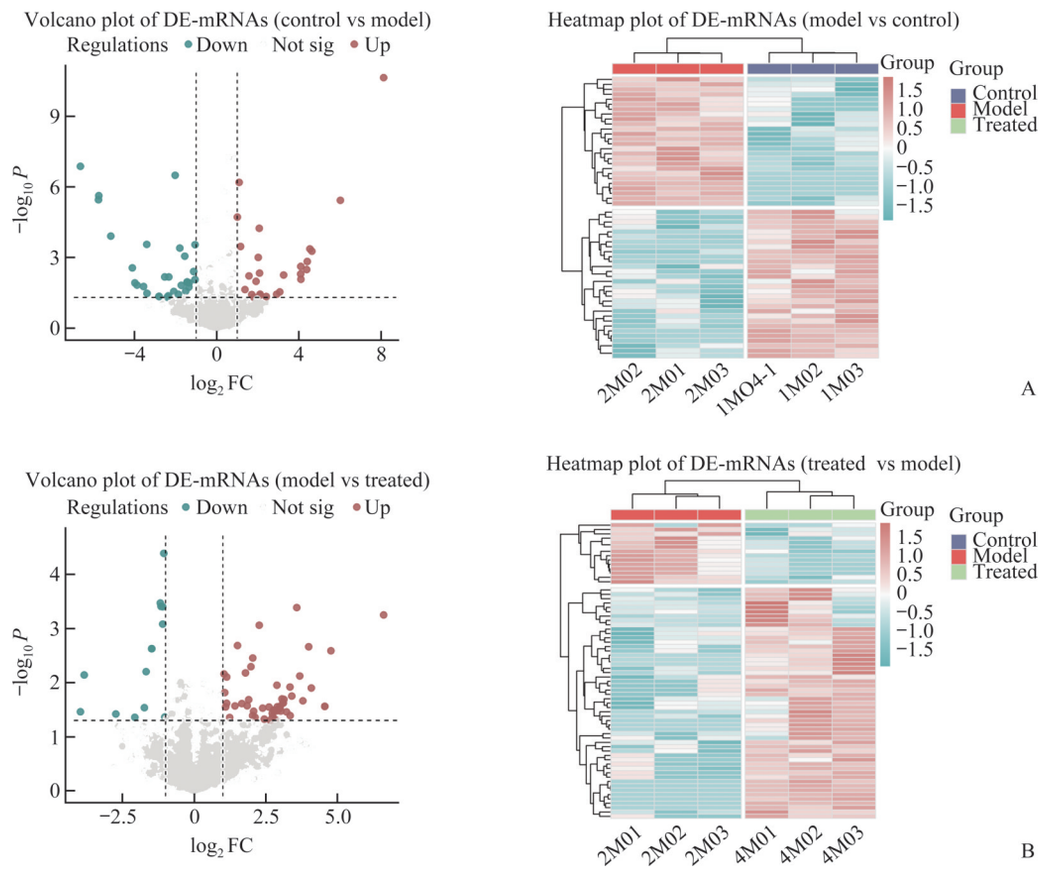

Figure 5 Differentially expressed miRNAs and functional analysis

A and B: Differentially expressed miRNAs between the control and model groups (A) and between the model and treated groups (B) are shown in volcano plots and hierarchical clustering heatmaps. Differentially expressed transcripts were screened using $|log_2FC|>1$ and $P<0.05$ as exploratory candidates for downstream analysis. NS: No significance.

The target genes of these lncRNAs were predicted. For the 55 lncRNAs that were significantly increased in the model group and significantly decreased after treatment, 270 targets were identified for 37 of them using cis-prediction, totaling 267 target genes. Trans-prediction resulted in 26 lncRNAs with 679 target relationships, with a total of 499 target genes (Supplementary Figure 4D, https://doi.org/10.57760/sciencedb.xbyxb.00168). For the 76 lncRNAs that were significantly downregulated within the model group but significantly upregulated after treatment, cis-prediction resulted in 76 lncRNAs with 406 target relationships, with a total of 390 target genes. Trans-prediction identified 58 lncRNAs with 1168 target relationships and 786 target genes (Supplementary Figure 4E, https://doi.org/10.57760/sciencedb.xbyxb.00168). Collectively, the 2 groups yielded 1 894 target genes (after deduplication of overlapping genes).

Metascape was then used for functional enrichment analyses. Supplementary Figure 5A (https://doi.org/10.

©Journal of Central South University (Medical Science). All rights reserved.

57760/sciencedb. xbyxb. 00168) shows that the target genes were mainly enriched in immune regulation, lymphocyte activation, wound healing, blood vessel remodeling, response to external stimuli, and myofibroblast differentiation. Also, eye vision functions, such as the canonical retinoid cycle in rods (twilight vision) and glutamatergic neuron differentiation, were involved. GO analysis showed the target genes were mainly enriched in negative regulation of neuroblast proliferation and integrin activation, metabolic enzyme and ion channel activities, as well as intermediate filament cytoskeleton and contractile ring (Supplementary Figure 5B, https://doi.org/10.57760/sciencedb.xbyxb.00168). KEGG pathway enrichment analysis showed that these target genes were mainly enriched in the forkhead box O (FoxO) pathway, retinoic acid-inducible gene I (RIG-I)-like receptor signaling pathway, longevity-regulating pathway (multiple species), non-alcoholic fatty liver disease, cytokine-cytokine receptor crosstalk, and phosphatidylinositol signaling system (Supplementary Figure 5C, https://doi.org/10.57760/sciencedb.xbyxb.00168).

2.5 Differentially expressed circRNAs and functional analysis

The original matrix contained 5 749 circRNA transcripts. After removal of low-abundance transcripts (sum count ⩽1 across all samples), 2 893 circRNAs were retained for downstream analysis. PCA showed a clear separation among the 3 groups based on circRNA expression profiles (Supplementary Figure 1J, https://doi.org/10.57760/sciencedb. xbyxb. 00168). Differential expression analysis was then performed using DESeq2 with $|\log_2 FC|>1$ and $P<0.05$ as an exploratory screening threshold. After normalization with DESeq2, the differential analysis of the expression matrix was conducted. Compared with the control group, 45 circRNAs were markedly decreased ($\log_2 FC<-1$, $P<0.05$) in the model group, and 47 were significantly increased ($\log_2 FC>1$, $P<0.05$) within model group (Supplementary Figure 6A, https://doi.org/10.57760/sciencedb.xbyxb.00168). In contrast, compared with the model group, 25 circRNAs were significantly decreased ($\log_2 FC<-1$, $P<0.05$) and 22 circRNAs were significantly increased ($\log_2 FC>1$, $P<0.05$) within the treated group (Supplementary Figure 6B, https://doi.org/10.57760/sciencedb.xbyxb.00168). CircRNAs whose expression was reversed after treatment were screened: 11 circRNAs were significantly downregulated in the model group but significantly upregulated following treatment. Meanwhile, 10 circRNAs were markedly upregulated in the model group but significantly downregulated after treatment (Supplementary Figure 6C, https://doi.org/10.57760/sciencedb.xbyxb.00168).

Next, the functions of the parental genes of these circRNAs were enriched using the clusterProfiler package. The biological process (BP) was mainly enriched in the modulation of synaptic neural signals and the transmission of second messengers, as well as transcriptional regulation (Supplementary Figure 6D, https://doi. org/10.57760/sciencedb. xbyxb. 00168). KEGG pathways included typical neural signaling pathways, such as calcium signaling and vascular endothelial growth factor (VEGF) signaling (Supplementary Figure 6E, https://doi.org/10.57760/sciencedb.xbyxb.00168).

2.6 Construction of the ceRNA regulatory network consisting of lncRNAs, circRNAs, and miRNAs

After differential expression analysis, ceRNA networks were constructed. First, 76 lncRNAs were downregulated in the model group, but upregulated after treatment, and 3 miRNAs (rno-miR-1-3p, novel_miR_1203, novel_miR_1417) were upregulated in the model group but downregulated after treatment, and were applied for correlation analysis using the Perl language code provided by TargetScan (TargetScan_70. pl), resulting in 474 interaction messages. The percentages of each interaction mode (8mer-1a, 7mer-m8, 7mer-1a, and 6mer) are shown in Supplementary Figure 7A (https://doi.org/10.57760/sciencedb.xbyxb.00168), and the 8mer-1a data were used for further analysis. The mRNA targets of the miRNAs were predicted. Based on predicted miRNA-binding sites and expression patterns, potential ceRNA networks were constructed, with 12 lncRNAs, 2 miRNAs, and 23 mRNAs obtained and shown in Supplementary Figure 7B (https://doi. org/10.57760/sciencedb. xbyxb. 00168). Second, 55 lncRNAs were upregulated in the model group but downregulated after treatment, and 2 miRNAs (novel_miR_107, novel_miR_905) were downregulated in the model group but upregulated after treatment were applied for correlation analysis using the Perl language code

©Journal of Central South University (Medical Science). All rights reserved.

provided by TargetScan (TargetScan_70.pl), resulting in 224 interaction messages. The percentage of each interaction mode is shown in Supplementary Figure 7C (https://doi.org/10.57760/sciencedb.xbyxb.00168). Similarly, the 8mer-1a information was used in subsequent analyses. Supplementary Figure 7D (https://doi.org/10.57760/sciencedb.xbyxb.00168) presents the analysis of miRNA target mRNAs; the ceRNA networks consisting of 14 lncRNAs, 1 miRNA (novel_miR_905), and 11 mRNAs were obtained.

Regarding circRNAs, 11 circRNAs decreased within the model group, while those that increased after treatment were analyzed together with the 3 miRNAs (rno-miR-1-3p, novel_miR_1203, and novel_miR_1417), which increased within the model group but decreased after treatment. After predicting the mRNA targets of the miRNAs, ceRNA networks consisting of 5 circRNAs (rno_circ_Rims2_10, rno_circ_intergenic_833, rno_circ_ Eif4enif1_3, rno_circ_Srpk2_2, and rno_circ_Akap6_2), 3 miRNAs, and 10 mRNAs (*Cdc167*, *Rnf152*, *Dpf3*, *Spry3*, *Tbp*, *Coil*, *Znhit3*, *Utp11*, *Dph6*, and *Sec62*) were obtained and shown in Supplementary Figure 7E (https://doi.org/10.57760/sciencedb.xbyxb.00168). Finally, 10 circRNAs upregulated in the model group but downregulated after treatment were analyzed together with the 2 miRNAs (novel_miR_905, novel_miR_107) decreased within the model group while increased after treatment. The mRNA targets of the miRNAs were predicted, and ceRNA networks consisting of 2 circRNAs (rno_circ_Ralgapa1_3 and rno_circ_March1_1), 2 miRNAs, and 8 mRNAs (*Mblac2*, *Rnft1*, *Dcbld1*, *Tob2*, *Lrp4*, *Trip13*, *Spred1*, and *Tmem47*) were obtained and shown in Supplementary Figure 7F (https://doi.org/10.57760/sciencedb.xbyxb.00168).

2.7 Real-time RT-PCR validation of treatment-reversed mRNAs

To further validate the sequencing-based mRNA expression profiles, 10 treatment-reversed mRNA (including *Med22*, *Rmt1*, *Sytl3*, *Itgb7*, *Slc1a3*, *Rnf183*, *Lrrc29*, *Lat2*, *Hist1h4m*, and *Dpm3*) were selected from the intersected differentially expressed mRNA sets for real-time RT-PCR analysis. These genes were selected because they showed marked changes in expression in the hypertensive retinopathy model group and opposite changes following lacidipine treatment. Among them, *Med22*, *Rmt1*, *Sytl3*, *Itgb7*, and *Slc1a3* were decreased in the model group compared with the control group. In contrast, their expression levels increased after lacidipine treatment (Figure 6). *Rnf183*, *Lrrc29*, *Lat2*, *Hist1h4m*, and *Dpm3* were increased in the model group compared with the control group. In contrast, their expression levels were decreased after lacidipine treatment (Figure 6).

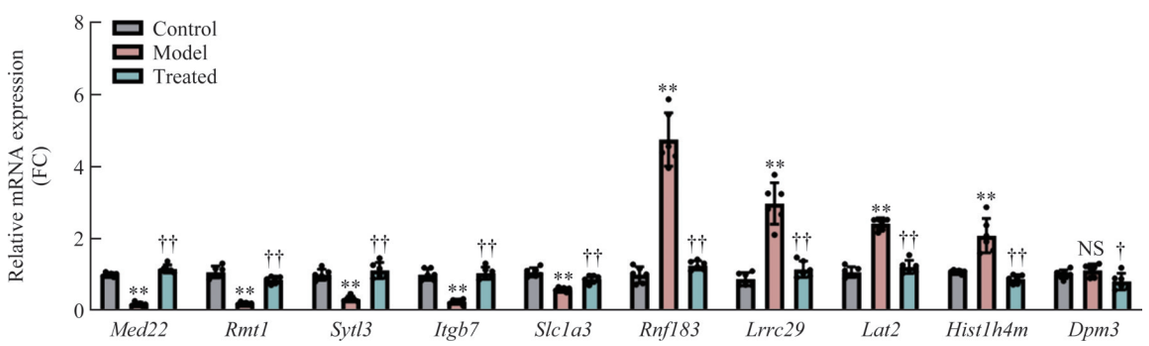

Figure 6 Real-time RT-PCR validation of selected treatment-reversed mRNAs

Expression levels of 10 selected mRNAs (*Med22*, *Rmt1*, *Sytl3*, *Itgb7*, *Slc1a3*, *Rnf183*, *Lrrc29*, *Lat2*, *Hist1h4m*, and *Dpm3*) were detected in retinal tissues from the control, model, and treated groups using real-time RT-PCR. Data are presented as the mean± standard deviation (n=6). The between-group comparisons are made by independent t-test. **P<0.01 compared to control group; ††P<0.01 compared to model group.

3 Discussion

This study investigated the molecular underpinnings of hypertensive retinopathy in a rat model, focusing on the differential expression of mRNAs, miRNAs, lncRNAs, and circRNAs. This study

©Journal of Central South University (Medical Science). All rights reserved.

characterized the transcriptomic landscape of retinal tissues in a spontaneously hypertensive rat model of hypertensive retinopathy and evaluated the treatment-associated molecular changes after lacidipine administration. Histopathological analysis confirmed retinal injury in the model group and partial improvement after treatment. Multi-layer RNA sequencing further revealed extensive alterations in mRNAs, miRNAs, lncRNAs, and circRNAs. More importantly, integrated enrichment analysis indicated that these RNA changes were not random but converged mainly on immune-inflammatory activation, oxidative and cellular stress responses, ECM remodeling, vascular and cell-adhesion pathways, and neuroretinal homeostasis. These processes are closely related to the recognized pathological features of hypertensive retinopathy, including retinal microvascular injury, inflammatory activation, vascular remodeling, and secondary neuronal dysfunction.

Rather than indicating isolated RNA changes, the transcriptomic profiles in the present study suggested 2 major biological themes in hypertensive retinopathy: Immune-inflammatory activation and disruption of neurovascular/retinal homeostasis. The mRNAs upregulated in the model group were mainly associated with leukocyte activation, chemotaxis, cytokine-related responses, oxidative stress, and immune-inflammatory signaling. In contrast, genes reduced in the model group were enriched in extracellular matrix organization, cell adhesion, vascular smooth muscle contraction, ion transport, and synaptic or glutamate-related processes. These findings are consistent with the pathological characteristics of hypertensive retinopathy, in which chronic elevation of blood pressure induces endothelial injury, vascular remodeling, impairment of the blood-retinal barrier, inflammatory cell recruitment, and secondary retinal neuronal stress[15]. Lacidipine treatment partially reversed these transcriptional alterations, suggesting that its protective effect may be associated not only with blood pressure control but also with attenuation of retinal inflammatory stress and restoration of neurovascular homeostasis.

Gene expression alterations are pivotal in the pathogenesis of hypertensive retinopathy. These alterations can result in the release of abnormal amounts of proteins, thereby disrupting the normal functioning of retinal cells and contributing to disease development. Understanding these alterations can provide valuable insights into the molecular mechanisms underlying hypertensive retinopathy, potentially paving the way for new therapeutic strategies[16]. In this study, mRNAs were found to be significantly decreased or increased in the hypertensive retinopathy model compared to the control group, and again post-treatment, highlighting the dynamic nature of gene expression under disease and treatment. The functional enrichment of differentially expressed mRNAs revealed their involvement in key biological processes, including changes in the immune microenvironment, cellular stress response, and tissue morphogenesis. Chemokines such as C-C motif chemokine ligand (CCL) 2, CCL4, C-X-C motif chemokine ligand (CXCL) 9, and CXCL10 have been found in the eyes of patients with diabetic retinopathy (DR) [17]. CXC chemokines recruit immune cells via attaching to C-X-C motif chemokine receptor (CXCR) 2, and CXCL1-CXCR2 signaling contributes to myocardial ischemia/reperfusion damage, high blood pressure, cardiac remodeling, and angiotensin II-induced ventricular fibrillation[18-19]. The KEGG signaling pathway enrichment also indicated that the upregulated mRNAs were involved in changes in the immune microenvironment, consistent with the recognized role of inflammation in hypertensive retinopathy[20-22] and with the GO functional annotation. The decreased mRNAs were shown to be associated with the PI3K/AKT signaling, a key pathway in hypertensive retinopathy[6, 23]. Notably, the effect of PI3K/AKT signaling on hypertensive retinopathy is also linked to inflammation, suggesting that genes altered in the immune microenvironment, as well as inflammatory changes, should be further investigated to elucidate their specific functions and mechanisms.

The real-time RT-PCR validation further supported the sequencing findings by confirming 2 major expression patterns among treatment-reversed mRNAs. *Med22*, *Rmt1*, *Sytl3*, *Itgb7*, and *Slc1a3* were reduced in the hypertensive retinopathy model and increased after lacidipine treatment. Conversely, *Rnf183*, *Lrrc29*, *Lat2*, *Hist1h4m*, and *Dpm3* were increased in the model group and decreased after treatment. Among these candidates, *Rnf183* and *Lat2* may be particularly relevant to stress-response and immune-inflammatory activation[24-25],

©Journal of Central South University (Medical Science). All rights reserved.

respectively, although their direct roles in hypertensive retinopathy require further functional validation. Rnf183, an E3 ubiquitin ligase associated with stress-related protein degradation[26], was markedly increased in the model group and reduced after lacidipine treatment, suggesting that endoplasmic reticulum stress-related ubiquitination and injury responses may be activated in hypertensive retinal tissues. *Lat2*, an adaptor molecule involved in immune receptor signaling[27], also showed a model-induced increase and a treatment-associated decrease, supporting the involvement of immune cell activation in hypertensive retinopathy. In contrast, *Slc1a3* was reduced in the model group and increased after treatment. Because *Slc1a3* encodes a major glutamate transporter that maintains extracellular glutamate homeostasis[28], its reduction might reflect impaired retinal neuroglial protection and increased susceptibility to excitotoxic stress. *Itgb7* was also decreased in the model group and partially restored after treatment, indicating that altered cell adhesion and immune cell trafficking may contribute to retinal vascular remodeling under hypertensive conditions[29]. These candidate molecules provide a more focused molecular framework linking the sequencing results to retinal vascular injury, inflammatory activation, and neurovascular dysfunction. However, their causal roles in hypertensive retinopathy and lacidipine-mediated protection require further mechanistic validation. Taken together, the functional enrichment results of differentially expressed RNAs and real-time RT-PCR validation results suggest that immune-inflammatory activation and impaired neurovascular homeostasis may represent 2 central molecular features of hypertensive retinopathy in this model, providing a focused molecular basis for interpreting the downstream non-coding RNA findings.

Among the predicted ncRNA candidates, rno_circ_Rims2_10 may be of particular interest because its parental gene, *Rims2*, is involved in synaptic vesicle exocytosis and neurotransmitter release[30]. In the retina, synaptic transmission between photoreceptors, bipolar cells, and downstream neurons is essential for maintaining visual signaling, and disruption of synaptic homeostasis may contribute to neurovascular dysfunction during retinal injury[31]. In the present study, rno_circ_Rims2_10 was included in a predicted treatment-responsive circRNA-miRNA-mRNA network, suggesting that synaptic regulation-related circRNAs may participate in the transcriptomic remodeling associated with hypertensive retinopathy. However, this interpretation remains hypothetical because the expression, cellular localization, and binding activity of rno_circ_Rims2_10 were not experimentally validated. Future studies should determine whether rno_circ_Rims2_10 is expressed in retinal neurons, glial cells, or vascular cells and whether it functionally regulates miRNA-dependent target gene expression under hypertensive retinal stress.

Consistent with the mRNA-level evidence, the miRNA results further suggested that post-transcriptional regulation may participate in inflammatory activation, cellular stress responses, and retinal neurovascular dysfunction in hypertensive retinopathy. MiRNAs are a class of small ncRNAs that exert a critical role in the post-transcriptional modulation of gene expression, and their dysregulation contributes to various diseases[32], including hypertensive retinopathy[9, 33]. For instance, dysregulation of miR-637 has been implicated in the progression of hypertensive retinopathy and in the regulation of retinal endothelial cell proliferation[34]. In addition, upregulated miR-194-5p has been reported to suppress dysfunction in retinal microvascular endothelial cells and mitigate hypertensive retinopathy symptoms in mice by targeting the SRY-box transcription factor 17 (SOX17) and VEGF pathways[5]. Herein, the expression levels of several miRNAs were significantly altered in the hypertensive retinopathy model compared with the control group, and in the treatment group compared with the model group, further supporting the notion that miRNAs may contribute to the development of hypertensive retinopathy and could serve as therapeutic targets. Regarding the mechanism of miRNA function, target genes were predicted and examined for functional and signaling pathway enrichment. The predicted targets of these differentially expressed miRNAs were mainly enriched in pathways associated with immune response, cellular stress response, and energy metabolism, among others. The immune response has been shown to contribute to vascular damage in hypertensive retinopathy[35], and cellular stress responses, particularly oxidative stress,

©Journal of Central South University (Medical Science). All rights reserved.

have been implicated in its pathogenesis[36].

The lncRNA-related findings also supported the involvement of immune regulation, wound healing, vascular remodeling, and responses to external stimuli, further linking non-coding RNA dysregulation to retinal inflammatory and vascular injury. LncRNAs are a class of ncRNAs that comprise more than 200 nucleotides and contribute to various biological activities and diseases, including hypertensive retinopathy[37]. LncRNAs have been reported to exert crucial effects on hypertension and cardiovascular disorders[38-39], and to play a vital role in the regulation of retinopathy[40]. However, for the specific role, *lncNALT* knockdown has been reported to ameliorate hypertensive retinopathy via the phosphatase and tensin homolog (PTEN)/PI3K/AKT signaling pathway[6]. Herein, various differentially expressed lncRNAs were identified in the hypertensive retinopathy model compared with normal controls, as well as in model rats after treatment, suggesting that additional lncRNAs may be involved in the pathogenesis of hypertensive retinopathy and could serve as therapeutic targets. Moreover, targets were also predicted and analyzed. The predicted targets of these differentially expressed lncRNAs were mainly enriched in pathways associated with immune regulation, wound healing, blood vessel remodeling, and responses to external stimuli. These findings further highlight the essential role of immune regulation and related genes and align with previous studies[35, 41] reporting that these pathways are involved in hypertensive retinopathy. As mentioned above, immune regulation and wound-healing processes have been shown to contribute to the vascular damage observed in hypertensive retinopathy[35], and blood vessel remodeling is a key feature of this condition[41].

In addition, the circRNA results extended these observations to regulatory processes involving neural signal modulation, second-messenger transmission, calcium signaling, and VEGF-related vascular responses. A significant number of differentially expressed circRNAs in hypertensive retinopathy were also identified, consistent with a previous study[42] reporting altered circRNA expression profiles in various diseases, including ocular disorders. Our analysis revealed that both types of circRNAs were significantly upregulated or downregulated in the model group, whereas they were downregulated or upregulated after treatment. This dynamic change in circRNA expression suggests a potential role on the pathogenesis of hypertensive retinopathy and treatment response. Functional enrichment analysis demonstrated that the parental genes of these differentially expressed circRNAs were involved in key biological processes, including neural signal regulation, second-messenger signaling, and transcriptional regulation, which are essential to the pathogenesis of hypertensive retinopathy[43-45]. Furthermore, KEGG pathway analysis highlighted the involvement of these circRNAs in calcium signaling and VEGF signaling. Calcium signaling has been shown to play a crucial role in neuronal function and survival, and its dysregulation is linked to various neurodegenerative diseases[46]. The VEGF signaling pathway, on the other hand, plays a critical regulatory role in angiogenesis and vascular permeability, and its dysregulation is a hallmark of many ocular diseases, including hypertensive retinopathy[47].

Together with the validated treatment-reversed mRNAs, the predicted ceRNA networks suggest that ncRNAs may provide an additional regulatory layer associated with immune-inflammatory activation, extracellular matrix remodeling, cellular stress responses, and neurovascular dysfunction in hypertensive retinopathy. As an exploratory component of the present study, ceRNA network analysis was performed to identify potential regulatory relationships among lncRNAs, circRNAs, miRNAs, and mRNAs; however, these predicted networks should be interpreted as candidate regulatory axes rather than evidence of direct causal interactions, which require further experimental validation. The concept of the ceRNA network has emerged as a novel layer of gene regulation, in which lncRNAs, circRNAs, and other ncRNAs may act as molecular sponges to sequester miRNAs, thereby modulating the expression of miRNA target genes[48-49]. This intricate network of RNA interactions has been implicated in various biological processes and disorders, including hypertension[50-51]. In the present study, treatment-responsive ceRNA networks provided a preliminary framework for exploring how ncRNAs may participate in transcriptomic alterations associated with hypertensive retinopathy. Several lncRNAs and circRNAs, including MSTRG. 23678.329,

©Journal of Central South University (Medical Science). All rights reserved.

MSTRG.183255.37, MSTRG.309824.28, rno_circ_Eif4enif1_3, rno_circ_Srpk2_2, and rno_circ_Akap6_2, were decreased in the model group but increased after lacidipine treatment, showing expression patterns opposite to those of rno-miR-1-3p, novel_miR_1203, and novel_miR_1417. The novel_miR_1417-related predicted targets, such as *Dpf3*, *Cdc167*, *Rnf152*, and *Spry3*, were functionally associated with chromatin remodeling, inflammatory or immune-related responses, ubiquitin-dependent signaling, and growth factor-related pathways[52-54], suggesting that this network may be involved in retinal stress responses and neurovascular remodeling after lacidipine treatment. This interpretation should therefore be considered exploratory. Since miR-1 has been reported to increase in retinal degeneration models[55], the increased rno-miR-1-3p level observed in the model group may reflect retinal stress responses under hypertensive conditions. In addition, several predicted target genes in these networks, including *Mmp14*[56-57], *Fasn*[58], and *Ext2*[59], have been previously associated with diabetic retinopathy, indicating that extracellular matrix remodeling, lipid metabolism, and glycosaminoglycan biosynthesis may be relevant to retinal injury-related molecular changes. In another treatment-responsive network, ncRNAs that were upregulated in the model group and downregulated after treatment were predicted to interact with novel_miR_905 and novel_miR_107, which showed the opposite expression pattern. Several predicted mRNA targets in this network also have potential relevance to retinal vascular biology and hypertension-related injury. For example, Gnai1 has been implicated in retinal neovascularization[60]. Low-density lipoprotein receptor-related proteins (LRPs) have been implicated in the development of pulmonary arterial hypertension (PAH)[61]. The deficiency of LRP1 in pulmonary arterial smooth muscle cells contributed to PAH[62]. The genetic polymorphism of LRP4 has been reported to be associated with hypertension[63]. In this study, *Lrp4* and *Spred1* were decreased in the model group and increased after lacidipine treatment, suggesting that these genes may be associated with treatment-related restoration of retinal vascular homeostasis. Collectively, these findings suggest that the predicted ceRNA networks may provide candidate regulatory relationships linking ncRNAs to inflammatory, extracellular matrix-related, metabolic, and vascular alterations in hypertensive retinopathy. Nevertheless, these interactions remain computationally predicted and require further experimental validation.

These findings indicate that part of the transcriptomic signature identified in the SHR model may overlap with molecular processes reported in other retinal vascular diseases, particularly diabetic retinopathy, including inflammation, extracellular matrix remodeling, metabolic dysregulation, and vascular remodeling. However, direct comparison with transcriptomic datasets from patients with hypertensive retinopathy was not performed in the present study; therefore, the clinical relevance of these candidate RNA signatures requires further validation in human retinal samples or publicly available human datasets. Several limitations should be acknowledged. First, although SHRs are commonly used to study hypertension-associated retinal injury, this model cannot fully reproduce the complexity and heterogeneity of human hypertensive retinopathy. Moreover, because lacidipine is a calcium channel blocker with antihypertensive activity, the transcriptomic changes observed after lacidipine treatment may reflect both direct drug-related effects on retinal cells and secondary effects associated with systemic blood pressure reduction, which cannot be fully distinguished in the current experimental design. Second, the ceRNA networks constructed in this study were based on bioinformatics prediction and expression correlation analysis. Although adjusted *P* values were applied to the mRNA and lncRNA differential expression analyses, miRNA and circRNA candidates were screened using nominal *P* values because strict FDR correction yielded very few or no candidates for downstream exploratory network analysis. Therefore, these networks cannot establish direct binding, regulatory direction, or causal effects among lncRNAs, circRNAs, miRNAs, and mRNAs. Further experimental validation, including luciferase reporter assays, RNA pull-down assays, RNA immunoprecipitation, loss- and gain-of-function experiments, and protein-level analyses, is required to confirm the predicted regulatory axes. In addition, representative treatment-responsive miRNAs, lncRNAs, and circRNAs should be further validated by real-time RT-PCR and spatially examined using in situ hybridization, while knockdown or overexpression assays in retinal vascular endothelial

©Journal of Central South University (Medical Science). All rights reserved.

cells, retinal pigment epithelial cells, or in vivo models would be needed to determine their functional roles in hypertensive retinal injury. Accordingly, the ceRNA-related and treatment-associated findings should be interpreted cautiously.

In conclusion, our study has provided a comprehensive view of the molecular mechanisms underlying hypertensive retinopathy, highlighting the significant roles of mRNAs, miRNAs, lncRNAs, and circRNAs. This study provides an integrated transcriptomic profile of mRNAs, miRNAs, lncRNAs, and circRNAs in retinal tissues from an SHR model of hypertensive retinopathy. The identified differentially expressed molecules and the constructed ceRNA networks not only shed light on the pathogenesis of hypertensive retinopathy but also suggest potential therapeutic targets for the future development of targeted treatment regimens.

Contributions: SHI Wen Research design, paper writing; XIAO Shiyuan Data collecting and analysis; BU Bing, HUANG Tianxin, and JIANG Yiran Experimental operation, paper modification; JIANG Wenmin Research design, paper supervision and revision. The final version of the manuscript has been approved and read by all authors.

Conflict of interest: The authors declare that they have no conflicts of interest to disclose.

References

[1] Wong TY, Mitchell P. Hypertensive retinopathy[J]. N Engl J Med, 2004, 351(22): 2310-2317. https://doi.org/10.1056/nejmra032865.

[2] Cheung CY, Ikram MK, Sabanayagam C, et al. Retinal microvasculature as a model to study the manifestations of hypertension[J]. Hypertension, 2012, 60(5): 1094-1103. https://doi.org/10.1161/HYPERTENSIONAHA.111.189142.

[3] Tso M, Jampol L. Pathophysiology of hypertensive retinopathy [J]. Ophthalmology, 1982, 89(10): 1132-1145. https://doi.org/10.1016/S0161-6420(82)34663-1.

[4] Klein R, Klein BE, Moss SE, et al. Hypertension and retinopathy, arteriolar narrowing, and arteriovenous nicking in a population[J]. Arch Ophthalmol, 1994, 112(1): 92-98. https://doi.org/10.1001/archopht.1994.01090130102026.

[5] Wan QQ, Liu HT, Xu YX, et al. Upregulated miR-194-5p suppresses retinal microvascular endothelial cell dysfunction and mitigates the symptoms of hypertensive retinopathy in mice by targeting SOX17 and VEGF signaling[J]. Cell Cycle, 2023, 22(3): 331-346. https://doi.org/10.1080/15384101.2022.2119514.

[6] Kang H, Huang D, Li H, et al. lncNALT knockdown ameliorates hypertensive retinopathy via PTEN/PI3K/AKT pathway[J]. Bioengineered, 2022, 13: 15003-15012. https://doi.org/10.1080/21655979.2023.2180591.

[7] Esteller M. Non-coding RNAs in human disease[J]. Nat Rev Genet, 2011, 12(12): 861-874. https://doi.org/10.1038/nrg3074.

[8] Liu Y, Taylor NE, Lu LM, et al. Renal medullary microRNAs in dahl salt-sensitive rats: miR-29b regulates several collagens and related genes[J]. Hypertension, 2010, 55(4): 974-982. https://doi.org/10.1161/hypertensionaha.109.144428.

[9] Kato M, Castro NE, Natarajan R. microRNAs: potential mediators and biomarkers of diabetic complications[J]. Free Radic Biol Med, 2013, 64: 85-94. https://doi.org/10.1016/j.freeradbiomed.2013.06.009.

[10] Yu B, Wang S. Angio-LncRs: LncRNAs that regulate angiogenesis and vascular disease[J]. Theranostics, 2018, 8 (13): 3654-3675. https://doi.org/10.7150/thno.26024.

[11] Chen X, Zhou R, Shan K, et al. Circular RNA expression profiling identifies glaucoma-related circular RNAs in various chronic ocular hypertension rat models[J]. Front Genet, 2020, 11: 556712. https://doi.org/10.3389/fgene.2020.556712.

[12] Liu C, Yao M, Li C, et al. Silencing of circular RNA-ZNF609 ameliorates vascular endothelial dysfunction[J]. Theranostics, 2017, 7(11): 2863-2877. https://doi.org/10.7150/thno.19353.

[13] Shi W, Meng Z, Luo J. Connexin 43 (Cx43) regulates high-glucose-induced retinal endothelial cell angiogenesis and retinal neovascularization[J]. Front Endocrinol, 2022, 13: 909207. https://doi.org/10.3389/fendo.2022.909207.

[14] Zhou Y, Zhou B, Pache L, et al. Metascape provides a biologist-oriented resource for the analysis of systems-level datasets[J]. Nat Commun, 2019, 10: 1523. https://doi.org/10.1038/s41467-019-09234-6.

[15] Tripathy K, Arsiwalla T. Hypertensive retinopathy[M]. Treasure Island (FL): StatPearls Publishing, 2026.

[16] Fang F, Zhuang P, Feng X, et al. *NMNAT2* is downregulated in glaucomatous RGCs, and RGC-specific gene therapy rescues neurodegeneration and visual function[J]. Mol Ther, 2022, 30 (4): 1421-1431. https://doi.org/10.1016/j.ymthe.2022.01.035.

[17] Kinuthia UM, Wolf A, Langmann T. Microglia and inflammatory responses in diabetic retinopathy[J]. Front Immunol, 2020, 11: 564077. https://doi.org/10.3389/fimmu.2020.564077.

[18] Wang L, Zhang YL, Lin QY, et al. CXCL1-CXCR2 axis mediates angiotensin II-induced cardiac hypertrophy and remodelling through regulation of monocyte infiltration[J]. Eur Heart J, 2018, 39(20): 1818-1831. https://doi.org/10.1093/eurheartj/ehy085.

[19] Zhang YL, Cao HJ, Han X, et al. Chemokine receptor CXCR-2 initiates atrial fibrillation by triggering monocyte mobilization in mice[J]. Hypertension, 2020, 76(2): 381-392. https://doi.org/10.1161/hypertensionaha.120.14698.

©Journal of Central South University (Medical Science). All rights reserved.

[20] Coban E, Nizam I, Topal C, et al. The association of low-grade systemic inflammation with hypertensive retinopathy[J]. Clin Exp Hypertens, 2010, 32(8): 528-531. https://doi.org/10.3109/10641963.2010.496519.

[21] Duarte DA, Silva KC, Rosales MAB, et al. The concomitance of hypertension and diabetes exacerbating retinopathy: the role of inflammation and oxidative stress[J]. Curr Clin Pharmacol, 2013, 8(4): 266-277. https://doi.org/10.2174/1574884711308040002.

[22] Wang S, Li J, Bai J, et al. The immunoproteasome subunit LMP10 mediates angiotensin II-induced retinopathy in mice[J]. Redox Biol, 2018, 16: 129-138. https://doi.org/10.1016/j.redox.2018.02.022.

[23] Yue JZ, Zhao X. GPR174 suppression attenuates retinopathy in angiotensin II (Ang II)-treated mice by reducing inflammation via PI3K/AKT signaling[J]. Biomed Pharmacother, 2020, 122: 109701. https://doi.org/10.1016/j.biopha.2019.109701.

[24] Okamoto T, Imaizumi K, Kaneko M. The role of tissue-specific ubiquitin ligases, RNF183, RNF186, RNF182 and RNF152, in disease and biological function[J]. Int J Mol Sci, 2020, 21(11): 3921. https://doi.org/10.3390/ijms21113921.

[25] Yang M, Wu W. The immune-related plasma protein LAT2 as a protective modulator in diabetic retinopathy: a Mendelian randomization study[J]. Front Endocrinol, 2025, 16: 1638661. https://doi.org/10.3389/fendo.2025.1638661.

[26] Wu YF, Li X, Jia JY, et al. Transmembrane E3 ligase RNF183 mediates ER stress-induced apoptosis by degrading Bcl-xL [J/OL]. Proc Natl Acad Sci U S A, 2018, 115(12): E2762-E2771[2025-09-07]. https://doi.org/10.1073/pnas.1716439115.

[27] Orr SJ, McVicar DW. LAB/NTAL/*Lat2*: a force to be reckoned with in all leukocytes?[J]. J Leukoc Biol, 2010, 89(1): 11-19. https://doi.org/10.1189/jlb.0410221.

[28] Albury CL, Sutherland HG, Lam AWY, et al. Identification of polymorphisms in *EAAT1* glutamate transporter gene *SLC1A3* associated with reduced migraine risk[J]. Genes, 2024, 15(6): 797. https://doi.org/10.3390/genes15060797.

[29] Neri P, Ren L, Azab AK, et al. Integrin β7-mediated regulation of multiple myeloma cell adhesion, migration, and invasion[J]. Blood, 2011, 117(23): 6202-6213. https://doi.org/10.1182/blood-2010-06-292243.

[30] Han YY, Kaeser PS, Südhof TC, et al. RIM determines Ca^{2+} channel density and vesicle docking at the presynaptic active zone[J]. Neuron, 2011, 69(2): 304-316. https://doi.org/10.1016/j.neuron.2010.12.014.

[31] Copenhagen DR. Synaptic transmission in the retina[J]. Curr Opin Neurobiol, 1991, 1(2): 258-262. https://doi.org/10.1016/0959-4388(91)90087-N.

[32] Bartel DP. microRNAs genomics, biogenesis, mechanism, and function[J]. Cell, 2004, 116(2): 281-297. https://doi.org/10.1016/S0092-8674(04)00045-5.

[33] Heggermont WA, Heymans S. microRNAs are involved in end-organ damage during hypertension[J]. Hypertension, 2012, 60(5): 1088-1093. https://doi.org/10.1161/hypertensionaha.111.187104.

[34] Yang WG, Su MX, Yu YL, et al. Dysregulation of miR-637 is involved in the development of retinopathy in hypertension patients and serves a regulatory role in retinol endothelial cell proliferation[J]. Ophthalmic Res, 2023, 66(1): 1-7. https://doi.org/10.1159/000514915.

[35] Guzik TJ, Hoch NE, Brown KA, et al. Role of the T cell in the genesis of angiotensin II-induced hypertension and vascular dysfunction[J]. J Exp Med, 2007, 204(10): 2449-2460. https://doi.org/10.1084/jem.20070657.

[36] Touyz RM, Briones AM. Reactive oxygen species and vascular biology: implications in human hypertension[J]. Hypertens Res, 2011, 34(1): 5-14. https://doi.org/10.1038/hr.2010.201.

[37] Quinn JJ, Chang HY. Unique features of long non-coding RNA biogenesis and function[J]. Nat Rev Genet, 2016, 17(1): 47-62. https://doi.org/10.1038/nrg.2015.10.

[38] Jusic A, Devaux Y. Noncoding RNAs in hypertension [J]. Hypertension, 2019, 74(3): 477-492. https://doi.org/10.1161/hypertensionaha.119.13412.

[39] Ghafouri-Fard S, Shirvani-Farsani Z, Hussen BM, et al. The key roles of non-coding RNAs in the pathophysiology of hypertension[J]. Eur J Pharmacol, 2022, 931: 175220. https://doi.org/10.1016/j.ejphar.2022.175220.

[40] Zhang Y, Cai SW, Jia YR, et al. Decoding noncoding RNAs: role of microRNAs and long noncoding RNAs in ocular neovascularization[J]. Theranostics, 2017, 7(12): 3155-3167. https://doi.org/10.7150/thno.19646.

[41] Intengan HD, Schiffrin EL. Vascular remodeling in hypertension: roles of apoptosis, inflammation, and fibrosis[J]. Hypertension, 2001, 38(3): 581-587. https://doi.org/10.1161/hy09t1.096249.

[42] Guo N, Liu XF, Pant OP, et al. Circular RNAs: novel promising biomarkers in ocular diseases[J]. Int J Med Sci, 2019, 16(4): 513-518. https://doi.org/10.7150/ijms.29750.

[43] Kang Q, Yang C. Oxidative stress and diabetic retinopathy: Molecular mechanisms, pathogenetic role and therapeutic implications[J]. Redox Biol, 2020, 37: 101799. https://doi.org/10.1016/j.redox.2020.101799.

[44] Gábriel R. Neuropeptides and diabetic retinopathy[J]. Br J Clin Pharmacol, 2013, 75(5): 1189-1201. https://doi.org/10.1111/bcp.12003.

[45] Reiner A, Fitzgerald MEC, Del Mar N, et al. Neural control of choroidal blood flow[J]. Prog Retin Eye Res, 2018, 64: 96-130. https://doi.org/10.1016/j.preteyeres.2017.12.001.

[46] Berridge MJ. Calcium signalling and psychiatric disease: bipolar disorder and schizophrenia[J]. Cell Tissue Res, 2014, 357(2): 477-492. https://doi.org/10.1007/s00441-014-1806-z.

[47] Campochiaro PA. Molecular pathogenesis of retinal and choroidal vascular diseases[J]. Prog Retin Eye Res, 2015, 49: 67-81. https://doi.org/10.1016/j.preteyeres.2015.06.002.

[48] Salmena L, Poliseno L, Tay Y, et al. A ceRNA hypothesis: the Rosetta stone of a hidden RNA language?[J]. Cell, 2011, 146(3): 353-358. https://doi.org/10.1016/j.cell.2011.07.014.

[49] Tay Y, Rinn J, Pandolfi PP. The multilayered complexity of ceRNA crosstalk and competition[J]. Nature, 2014, 505(7483):

©Journal of Central South University (Medical Science). All rights reserved.

344-352. https://doi.org/10.1038/nature12986.

[50] Zhou H, Wang B, Yang Y, et al. Long noncoding RNAs in pathological cardiac remodeling: a review of the update literature[J]. BioMed Res Int, 2019, 2019: 7159592. https://doi.org/10.1155/2019/7159592.

[51] Han Y, Jin G, Pan M, et al. Integrated bioinformatics and validation of lncRNA-mediated ceRNA network in myocardial ischemia/reperfusion injury[J]. J Immunol Res, 2022, 2022(1): 7260801. https://doi.org/10.1155/2022/7260801.

[52] Cui H, Yi H, Bao H, et al. The SWI/SNF chromatin remodeling factor DPF_3 regulates metastasis of ccRCC by modulating TGF-β signaling[J]. Nat Commun, 2022, 13: 4680. https://doi.org/10.1038/s41467-022-32472-0.

[53] Kamptner A, Mayer C, Sutterlüty H. Sprouty3, but not Sprouty1, expression is beneficial for the malignant potential of osteosarcoma cells[J]. Int J Mol Sci, 2021, 22(21): 11944. https://doi.org/10.3390/ijms222111944.

[54] Zhang X, Jiang Q, Deng W, et al. RNF152-mediated, ubiquitin-dependent degradation of HSP27 activates the PI3K/AKT pathway, driving synovial inflammatory cascades in TMJOA [J]. Arthritis Res Ther, 2025, 28(1): 16. https://doi.org/10.1186/s13075-025-03715-4.

[55] Loscher CJ, Hokamp K, Wilson JH, et al. A common microRNA signature in mouse models of retinal degeneration [J]. Exp Eye Res, 2008, 87(6): 529-534. https://doi.org/10.1016/j.exer.2008.08.016.

[56] Abu El-Asrar AM, Mohammad G, Allegaert E, et al. Matrix metalloproteinase-14 is a biomarker of angiogenic activity in proliferative diabetic retinopathy[J]. Mol Vis, 2018, 24: 394-406. https://pmc.ncbi.nlm.nih.gov/articles/PMC5957543/.

[57] Ünal A, Baykal O, Öztürk N. Comparison of matrix metalloproteinase 9 and 14 levels in vitreous samples in diabetic and non-diabetic patients: a case control study[J]. Int J Retina Vitreous, 2022, 8(1): 44. https://doi.org/10.1186/s40942-022-00394-0.

[58] Gu CF, She XP, Zhou CD, et al. Dihydroartemisinin ameliorates retinal vascular dysfunction in diabetes mellitus via the FASN/Kmal-mTOR/SREBP1 feedback loop[J]. Pharmacol Res, 2021, 174: 105871. https://doi.org/10.1016/j.phrs.2021.105871.

[59] Rangasamy S, Monickaraj F, Legendre C, et al. Transcriptomics analysis of pericytes from retinas of diabetic animals reveals novel genes and molecular pathways relevant to blood-retinal barrier alterations in diabetic retinopathy[J]. Exp Eye Res, 2020, 195: 108043. https://doi.org/10.1016/j.exer.2020.108043.

[60] Sun J, Huang W, Yang SF, et al. Gαi1 and Gαi3mediate VEGF-induced VEGFR2 endocytosis, signaling and angiogenesis[J]. Theranostics, 2018, 8(17): 4695-4709. https://doi.org/10.7150/thno.26203.

[61] Calvier L, Herz J, Hansmann G. Interplay of low-density lipoprotein receptors, LRPs, and lipoproteins in pulmonary hypertension[J]. JACC Basic Transl Sci, 2022, 7(2): 164-180. https://doi.org/10.1016/j.jacbts.2021.09.011.

[62] Calvier L, Boucher P, Herz J, et al. LRP1 deficiency in vascular SMC leads to pulmonary arterial hypertension that is reversed by PPARγ activation[J]. Circ Res, 2019, 124(12): 1778-1785. https://doi.org/10.1161/CIRCRESAHA.119.315088.

[63] Park H, Jeon T, Kim Y, et al. Genetic polymorphisms of *ARMC4, LRP4* and *BCL2* genes are associated with blood pressure traits and hypertension in Korean population[J]. Biomed Sci Lett, 2020, 26(1): 28-36. https://doi.org/10.15616/bsl.2020.26.1.28.

(Edited by WU Xufang)

©Journal of Central South University (Medical Science). All rights reserved.